TID-4500, UC-35
Nuclear Explosions—
Peaceful Applications

Lawrence Radiation Laboratory
UNIVERSITY OF CALIFORNIA
LIVERMORE

UCRL-50951

THE HANDCAR NUCLEAR EXPLOSION IN DOLOMITE

Glenn C. Werth, Editor

Foreword

The publication of this report was unfortunately delayed by a number of factors including classification problems. It was not possible to resolve the classification issue except by publishing both classified and unclassified reports (UCRL-50967 and UCRL-50951, respectively). Some of the material in this report has become dated, but it is in the best interest of the Plowshare Program that it be published for the record. The report has been updated where practicable by appropriate revision to the text and by citation of recent publications.

Contents

THE HANDCAR NUCLEAR EXPLOSION IN DOLOMITE

Abstract

The Plowshare Program has continued its study of underground explosion processes with the detonation of a 12 ± 1 kt nuclear explosion in dolomite on November 5, 1964. This experiment, called the Handcar Event, was the first underground explosion in which a permanent gas (carbon dioxide) was generated in large quantities. Heretofore, underground explosions in carbonate rocks had been subject to considerable uncertainty because of the possible effect of the gas pressure on the stemming and safety of such a shot.

The Handcar nuclear explosive was emplaced in a 61-cm-diam hole cased with iron and stemmed with pea gravel and three grout plugs. It was fired in a thick dolomite section at a total depth of 462 m. The dolomite extended 157 m above the shot point and was overlain by 235 m of shale, alluvium, and tuff. The rock in the immediate vicinity of the shot point was about 99% dolomite, or $CaMg(CO_3)_2$, plus small amounts of impurities such as quartz, water, iron oxide, and calcite. It had been highly fractured by natural mechanisms and had a fracture porosity of 2% with a correspondingly high permeability. The stemming held and there were no measurable leaks of radioactivity to the surface through the medium, although trace amounts of gas leaked through instrument cables.

Logging of three postshot holes and pressurization of the chimney revealed that the explosion produced a cavity with a radius of approximately 21.2 m. This radius is about 14% less than would be expected for an explosion of the same yield in granite. This is consistent with the previously advanced hypothesis that water content of the shot environment is a dominant factor in cavity growth. The cavity partially collapsed and produced a rubble-filled chimney 68 m high (3.2 times the cavity radius) above the shot point. This height is about 27% less than that expected on the basis of results from explosions in fractured granite. The coincidence of the chimney apex with a major change in rock character indicates an influence of natural inhomogeneities on chimney growth.

Peak pressure measurements of 100-300 kbar at distances of 9, 10, and 13 m from the shot point are within 20% of preshot estimates. Stress history measurements of about 10 kbar at 45 m agree with calculations to within 25%. Below 5 kbar (beyond 50 m), however, experimentally observed amplitudes were a factor of 2 or 3 below the theoretical predictions. The long-range seismic signal was likewise a factor of 3 or 4

below that expected. The reasons for this are not known, but shock-wave energy losses in fractured materials in the nonlinear zone may be responsible.

About $(9 \pm 7) \times 10^8$ liters of CO_2 (at STP) was generated by the heat of the explosion. This decomposition of carbonate rock required 20 ± 15% of the energy of the explosion. In this experiment, the CO_2 generated by decomposition of carbonate rock did not compromise stemming and did not contribute to cavity growth.

Radiochemical analyses were made on both solid and gaseous samples. No indication was observed of any gross difference between dolomite and previously studied rocks in the retention of volatile and refractory radionuclides in the rock melt. Gas samples from the chimney region were about one-third air and two-thirds carbon dioxide, with trace quantities of methane, hydrogen, and carbon monoxide. Implications drawn from the specific activity of carbonaceous gases suggest that between 327 and 670 tons of dolomite per kiloton yield participated in carbon 14 exchange. Using ^{85}Kr totals as inferred from device yield measurements, one can calculate the totals of various species mixed with ^{85}Kr. Production of ^{37}Ar was 10^3 Ci/kt, and ^{39}Ar was 120 mCi/kt. The ratio of fission product gases is anomalous, the xenon isotopes being twice the ^{85}Kr in chimney gas. No completely satisfactory explanation is offered. However, the ratio of krypton to xenon is indicative of a rapid chimney depressurization as might be expected in the fractured dolomite matrix.

Introduction

Prior to Handcar, nuclear explosion experiments had been conducted only in silicate-base rocks (such as tuff and granite) and in salt. Through these experiments methods were developed for predicting cavity size and estimating chimney dimensions as well as the minimum depth of burial necessary to prevent dynamic venting. It was also found experimentally that most of the nongaseous fission products are scavenged by the melted silicate or salt, which subsequently solidifies and traps the radioactivity within it.

Extrapolation of data from explosions in silicates to carbonate-base rocks such as limestone and dolomite was open to serious question prior to Handcar. Carbonate rocks decompose when heated, releasing large quantities of carbon dioxide. How much gas would be released? What role would it play in dynamic growth of the cavity and containment? What is the strength of the seismic signal?

Because of these technical questions, it was not considered advisable to plan industrial applications of nuclear explosives at sites containing appreciable amounts of carbonate; hence, the need for the Handcar experiment. Also, such a contained experiment was a necessary prelude to a cratering experiment in carbonate rock.

The purpose of this report is to present the principal results of the Handcar experiment. References are made to previous reports which should be consulted to support the methods of analysis. The technical information in each of the sections has been prepared by members of the Plowshare staff of Lawrence Radiation Laboratory, and their contributions are acknowledged at the heading of each section.

Part I. Physics and Geology

(Coordinated by Glenn C. Werth)

GEOLOGIC ENVIRONMENT OF HANDCAR

Charles R. Boardman, David D. Rabb

A buried mountain ridge of Paleozoic dolomite at the Nevada Test Site was chosen as the location for the Handcar experiment. The configuration of the ridge and the cover of Cenozoic tuff and alluvium are depicted in Fig. 1. These sections are based on data from drill hole logs, cores, and gravity and seismic reflection surveys (USGS and Sandia Corporation). The bulk density (ρ) and compressional velocity (α) for each unit are given in the figure.

The shot point is located 402 m below ground surface, and 167 m below the top of the dolomite. Preshot physical properties of the dolomite are given in Table 1.

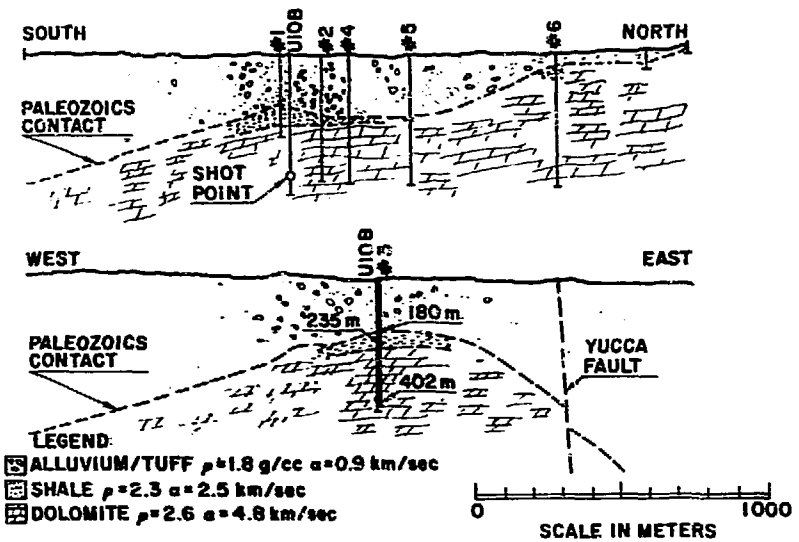

Fig. 1. Geologic cross sections of Handcar site.

Table 1. Preshot physical properties of Handcar dolomite.

Fractures

The Handcar dolomite is highly fractured, containing up to 95 fractures per meter of core length. These fractures form an interconnecting network, with the high-angle fracture planes (relative to the horizontal) outnumbering lower angle fracture planes by about 2 to 1.

Densities

Average *in situ* bulk density (borehole density log): 2.72 g/cc.

Average bulk density of core samples (laboratory measurement): 2.78 g/cc.

Average crystal density of core samples (laboratory measurement): 2.85 g/cc.

Porosity

The difference between the bulk density of core samples and the crystal densities of these samples indicates an intergranular porosity of about 3%.

The difference between the bulk density of core samples and the *in situ* bulk densities also indicates a porosity associated with fractures of 2%.

Permeability

Air injection tests verified connection between holes 122 m apart and indicated fracture permeabilities of 135-300 mD (millidarcys).

Static water table depth

The water table depth is estimated to be at 600 m (198 m below the shot point), based on well data 2 km southwest.

OPERATIONAL ASPECTS

John Toman

The depth of the explosion was chosen such that the chimney and most of the fracturing above the chimney would be in dolomite. Also, since the purity of the dolomite varies with depth, a particularly pure interval of better than 98 wt% $CaMg(CO_3)_2$ was selected in order to simplify the chemical analysis of the results. These two criteria served to determine the shot depth at 402 m. The maximum chimney height and fracturing radii were estimated from experience in other media (Boardman et al.[1]).

Prior experience with the containment of underground nuclear explosions in hard rock has shown that a 100-m buffer zone (ground surface to top of chimney) is a suitable criterion for containment. However, in alluvium a scaled depth of 107 $W^{1/3}$ meters is the criterion, where W is the number of kilotons of yield. The medium surrounding the shot point is hard rock overlain by alluvium. By either of the previously used criteria, Handcar was sufficiently deep to avoid dynamic venting and be contained. A

discussion of current containment criteria is presented by Germain and Kahn.[2] They report that, subsequent to Handcar, one nuclear event in saturated dolomite had some significant leakage.

A view of the Handcar nuclear explosive with its associated cabling is shown in Fig. 2. It had a diameter of 38 cm and a length of approximately 4.2 m. The emplacement hole was cased to a depth of 413 m with 61-cm-i.d. steel casing to prevent sloughing in the hole. Casing is not required in Plowshare applications if the test medium is competent. A smaller hole could have been used for Handcar.

Fig. 2. Handcar nuclear explosive canister and cables ready for lowering into the emplacement hole.

The emplacement procedure began on October 28, 1964. The explosive was lowered with flat wire rope at a rate controlled primarily by the requirement to tie on 14 electrical cables and grout pipes. The entire downhole package weighed about 13,600 kg. Eight hours were required to emplace the explosive at the zero point.

Dolomite chips were placed above the explosive to a height of 15.3 m in order to reduce the amounts of silicates surrounding the shot point and thus simplify the postshot chemical analysis. Above the dolomite chips, pea gravel alternating with three grout plugs, each 15.3 m in length, filled the emplacement hole. The grout plugs prevented the pea gravel, after the shot, from sliding down the emplacement hole either into the cavity or into the void at the top of the chimney, and acted as a barrier against migration of the cavity gases up the porous pea-gravel stemming.

The instrument layout at the Handcar site is shown in Fig. 3. The shock wave recording in holes U10b-1, -2, -4, -5, and -6 was done by Sandia under contract to the Defense Atomic Support Agency. The strong-motion seismic stations were operated by the U.S. Coast and Geodetic Survey under contract to Lawrence Radiation Laboratory (LRL). The remaining instruments were operated by the technical staff of LRL. Radiation monitoring teams were provided by Reynolds Electric and Engineering Company (REECo). The program was under the technical direction of LRL. Construction, safety, and test management was provided by the Nevada Operations Office of the Atomic Energy Commission.

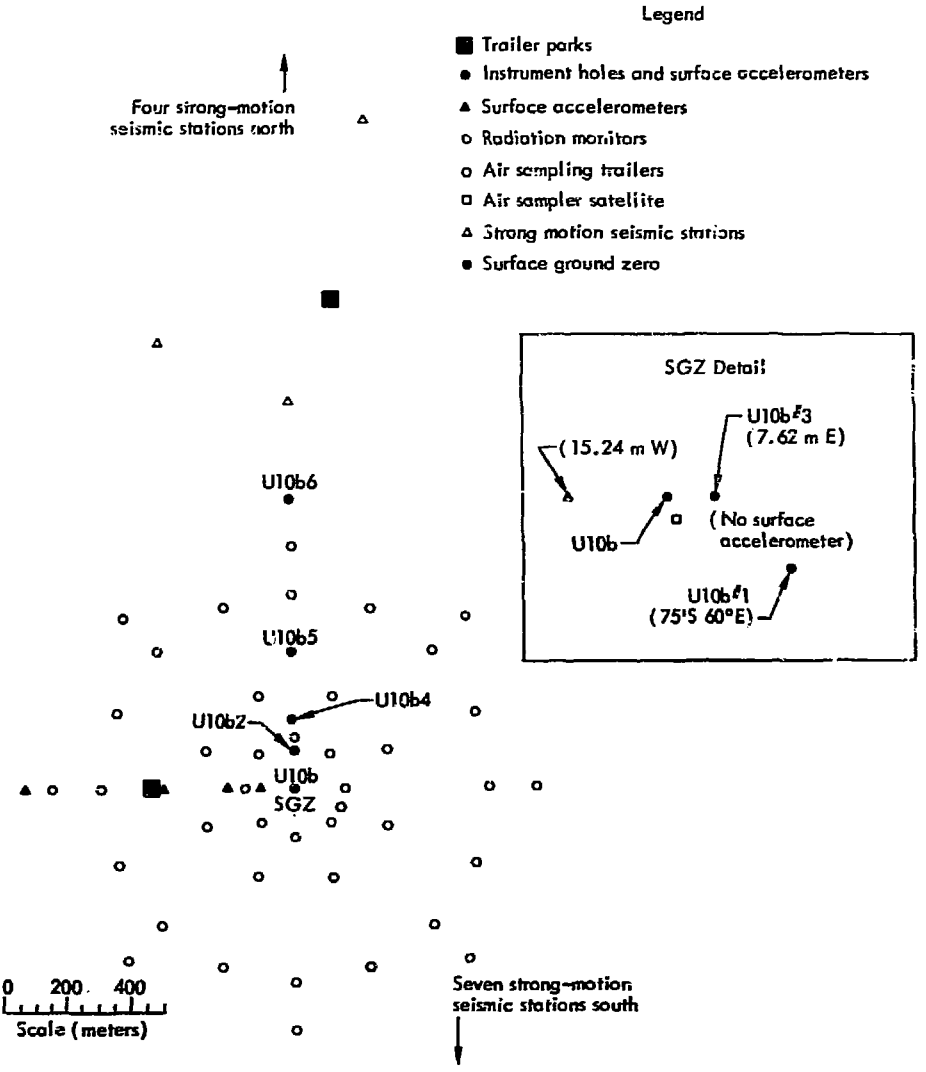

Fig. 3. Instrument layout at Handcar site.

The Handcar explosive was detonated at 0700:00.109 ± 1 msec, PST, November 5, 1964 (or 1500:00.109 ± 1 msec, GMT), at 37° 10' 27.7376" North Latitude and 116° 04' 01.3109" West Longitude. Nevada State coordinates of the zero point were N 882,999.17, E 674,704.06, at elevation 3055 ft above MSL. This

location is at the northern end of Yucca Valley. The planned yield was 11 kt. The total energy deposited, including secondary effects, was 12 ± 1 kt. With the exception of minor surface fracture sets there was no visual indication at the surface of a subsurface detonation. Geophone records indicated cavity collapse occurred and was arrested within 35 sec of the explosion.

There was no visual evidence of dynamic venting, and hence the Handcar explosion was considered to be contained. Minor seepage of radioactive gases did occur, but only through electrical cables. At H + 40 min a radiation monitor team entered the trailer area and recovered scientific data. By H + 1 hr 40 min the team had completed surveying the ground to an area within 153 m from surface ground zero, and no levels of radiation above background were found. As expected, a very small amount of activity was detected on a 26-pair cable originating at shot depth in the emplacement hole. The contact reading was 120 mR/hr. These cables were cut and partially sealed to stop the leak, as is the usual practice. The activities were identified as $^{87,88}Kr$ and ^{135}Xe. At H + 4 hr, a contact reading of 10 mR/hr was observed on a cable originating at shot level in instrument hole U10b-2, 122 m north of surface ground zero. This leak indicated significant lateral migration of the cavity gases through the fractured dolomite. Between H + 17 and 24 hr, traces of ^{135}Xe were detected with the air sampler units. During this period, radiation readings on the emplacement hole cable decreased to background. The total radioactivity released to the atmosphere is judged to be less than 200 Ci, a quantity so small and over such a long period that at no time did a health hazard exist.

POSTSHOT ENVIRONMENT

Charles R. Boardman, Lewis Meyer

The postshot environment was explored via slant holes PS #1A and PS #1A Whipstock, in December 1964, and via vertical hole PS #1V in November 1965. Figure 4 shows the cross section interpreted from the drilling data. Figure 5 is a photograph taken by a downhole camera at the top of the chimney rubble.

The average radius of the cavity generated by the explosion is 21.2 m. This radius is defined by the maximum radial extent of intense gamma radiation in the lower portion of the chimney. The average chimney void volume, as determined by pressurization, is about 36,200 m^3. The radius of an equivalent spherical volume is about 20.6 m.

Comparison of this radius with those obtained from explosions in other media is interesting. Experience has shown that, in the first approximation, the cavity expands adiabatically to the overburden pressure. The following equation is the relationship between yield W,

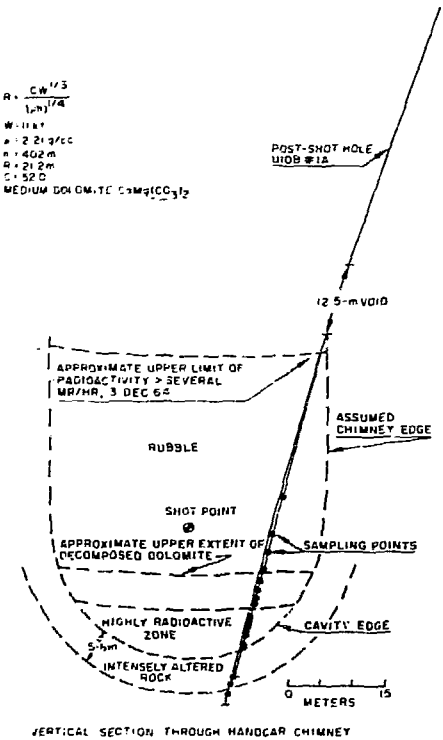

Fig. 4. Cross section of Handcar cavity based on postshot drilling.

average overburden density ρ, shot depth h, cavity radius R, and an empirical constant C (Boardman et al.[1]):

$$R = C \frac{W^{1/3}}{(\rho h)^{1/4}} .$$

The equation is plotted using a number of values for C in Fig. 6.

Handcar yielded a cavity radius 14% smaller than would be expected for an explosion of similar yield and overburden pressure in granite. This suggests that the formation of CO_2 gas did not play a major role in cavity formation. It is also consistent with the previously advanced hypothesis that the water content of the rock is the most important single factor in controlling cavity radius (see the table in Fig. 6). The lines shown in the figure are based on many experiments at the Nevada Test Site. The unclassified data, as can be seen, only marginally verify the relationship.

A zone of crushed rock extends 5-6 m below the bottom of the collapsed cavity ("intensely altered rock" zone in Fig. 4). The samples recovered in this region were chalky and friable. Below this region the sampling tool could not penetrate the more competent dolomite.

The maximum observed chimney height above shot point is 68 m, or 3.2 times the cavity radius. This value is about 27% less than the expected value of 4.2 times the cavity radius based on Shoal and Hardhat results. The coincidence of the chimney apex with a change in rock characteristics suggests the influence of nature's inhomogeneities on chimney growth. Subsequent calculations by Cherry et al.[3] indicated good agreement between the calculated extent of cracking and the measured height of the Handcar chimney.

The maximum observed chimney radius above the shot point is 28 m, or about 1.3 cavity radii. The annular shell of crushed dolomite probably failed upon collapse of the cavity, thus allowing the chimney radius to enlarge to this value.

The average percent voids of the chimney is 26%, based on the inferred cross section in Fig. 4 and the average volume of void determined by pressurization. The percent voids of the rubble is less than 20%, since the apical void

Fig. 5. Rubble at top of chimney, photographed by downhole camera.

represents a large fraction of the chimney void. This is consistent with a rather massive collapse occurring within 35 sec which would inhibit bulking.

The statistical analysis of particles observed by stereophotography (see Fig. 5) on the floor of the apical cavity indicates the following:

1. Median particle diameter by particle volume is 20 cm.

2. About 82% of the rubble volume is composed of particles with

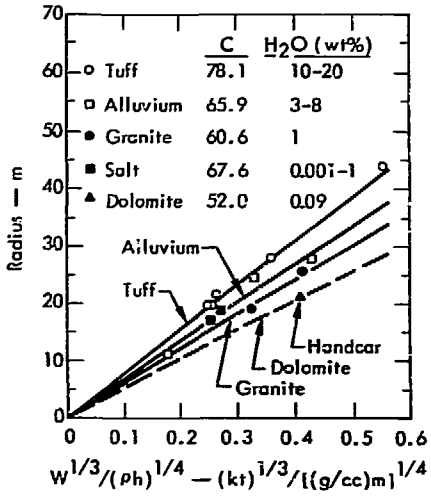

Fig. 6. Plots of scaling equation, $R = C(W^{1/3})(\rho h)^{-1/4}$, for various values of C. R is radius of cavity produced by a nuclear explosive of W kilotons yield in a medium of density ρ at a depth of h meters.

diameters in the range of 2.5 to 42.5 cm.

3. Maximum observed particle diameter is about 90 cm.

These statistics lend credence to the previously advanced hypothesis that the frequency of natural fractures is a major determinant of rubble particle size.

The highly radioactive zone shown in Fig. 4 yielded samples with gamma radiation levels several orders of magnitude greater than those higher in the chimney. The most highly radioactive sample recovered had a contact gamma radiation level of 10 R/hr 35 days after the explosion.

The maximum observed radial extent of low-level gamma radioactivity not associated with radioactive gases was 94 m above the shot point. The maximum observed level in the apical volume above the chimney rubble was 28 μR/hr measured in November 1965.

Approximately 5660 m^3 of drilling fluid was pumped into the chimney region during postshot exploratory drilling. Consequently, hole temperatures were abnormally low when logged 28 days after the explosion. A peak temperature of 54°C was observed near the base of the collapsed cavity. At shallower depths, but within the collapse chimney, hole temperatures averaged about 12°C above ambient. In November 1965, a year after the shot, the average air temperature in the apical void of the chimney was 34.5°C, or about 10°C above ambient. At this time, a break in the thermal gradient was observed at a radial distance of 113 meters above the shot point.

A complete report of the postshot cavity and chimney exploration was published by Boardman et al.[4] (1966).

SHOCK FRONT STUDIES

Leo A. Rogers

An understanding of the outgoing shock wave and seismic wave from a nuclear explosion is vital to Plowshare. In industrial applications, such as gas stimulation and copper leaching, nuclear explosions are useful only when they increase permeability by crushing and cracking rock. In cratering applications, the

breaking up of overburden material by the explosion shock wave is a preparatory step to lifting and ejecting the material to make a crater.

Figure 7 shows the variability in compressional and shear velocity of the Handcar medium with depth. On the basis of this data and density information, the medium above the detonation was divided into the six zones whose average properties are listed in Table 2. Prior to making theoretical calculations of the shock front, other rock properties must also be measured. Compressional and shear velocities, tensile and shear strengths, pressure-volume relationships (Fig. 8), and the elastic precursor must be measured. A general discussion of shock-compressed rock properties is contained in the paper by Rogers.[5] The Hugoniot data was measured by

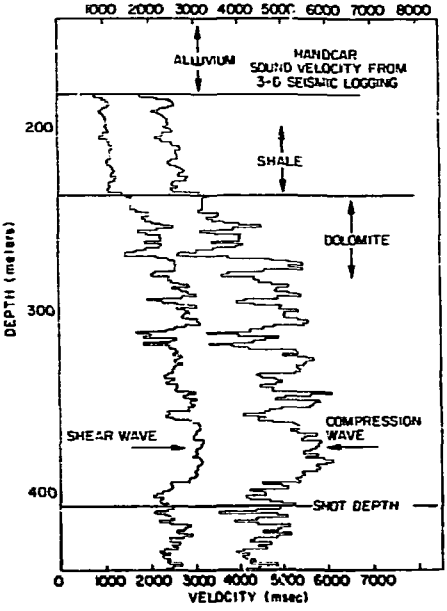

Fig. 7. Variation in sonic wave velocity with depth at the Handcar site.

Table 2. Input parameters for SOC calculations of Handcar.

Parameter	Alluvium	Shale	Mixture	Dolomite I	Dolomite II	Dolomite III
Density (g/cc)	1.7	2.19	2.63	2.59	2.65	2.59
Bulk modulus (kbar)	15.6	98.4	193	273	419	473
Shear modulus (kbar)	5.14	26.4	91.1	162	165	224
Tensile strength (kbar)	0	0	0	0.1	0.1	0.1
K_1 (kbar)	0	0.1	0.1	5	5	5
K_2 (kbar)	0	0.1	0.1	1.0	0.1	0.1
K_3 (kbar)	0	0.1	0.1	0.5	0.5	0.5
Y_0 (kbar)	10	100	100	1000	1000	1000
Y_1 (kbar)	0.5	1.0	1.0	0.5	1.0	2.0
Γ	1.0	1.0	1.0	1.0	1.0	1.0

K_1 = stress difference maximum for fast rising front.

K_2 = stress difference maximum for slowly rising front.

K_3 = stress difference maximum for crushed material.

Y_0 = crushing strength for solid material (confined).

Y_1 = crushing strength for cracked open material (unconfined).

Γ = Grüneisen parameter.

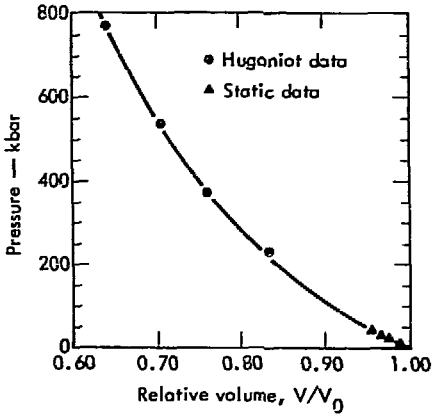

Fig. 8. Compressibility of Handcar dolomite.

LeRoy Hord (LRL, personal communication) and the static compressibility by Douglas Stephens (LRL personal communication).

The theoretical calculations were made with the Plowshare SOC code. Theoretical-experimental comparisons for nuclear explosions in granite, salt, tuff, alluvium, and dolomite are given by Holzer.[6] The vertical cross section, including the shale and alluvium, forms the spherically symmetric model for the calculation. Locations of the various experimental measurements made by LRL are given in Fig. 9. Results of these measurements and comparison with theory for the close-in hydrodynamic range are given in Figs. 10 and 11. In this close-in hydrodynamic region, we achieved excellent agreement between theory and experiment.

The theoretical values of tangential stress at 45 m are in reasonable agreement with the measured values (Fig. 12). But at 63 m, the calculated values for both the tangential stress, Fig. 13, and radial stress, Fig. 14, are at considerable variance with the experimental data.

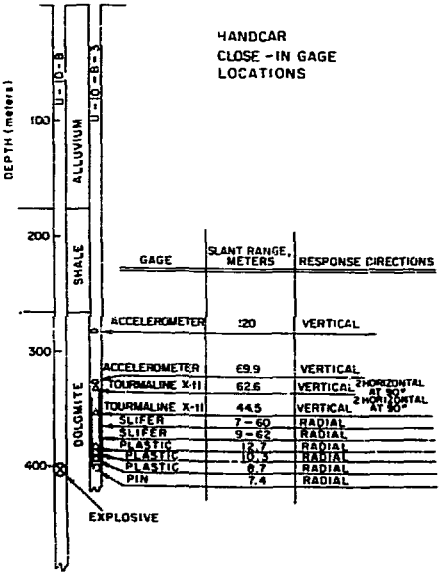

Fig. 9. Locations of LRL experimental measurements in Handcar.

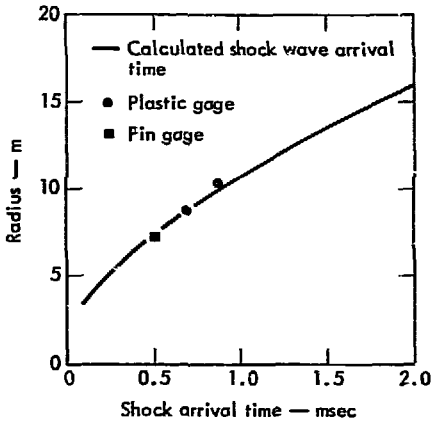

Fig. 10. Predicted and measured values for close-in shock arrival time.

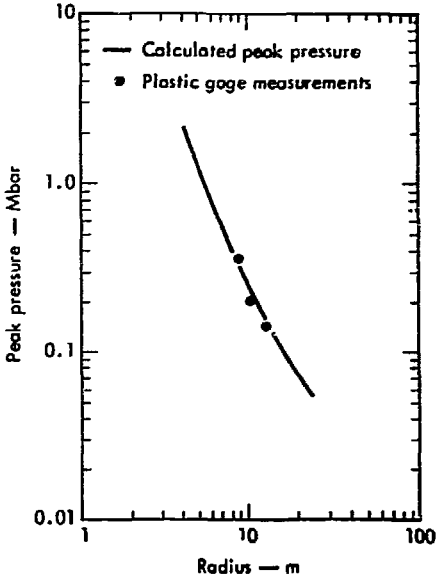

Fig. 11. Predicted and measured values of close-in peak pressures.

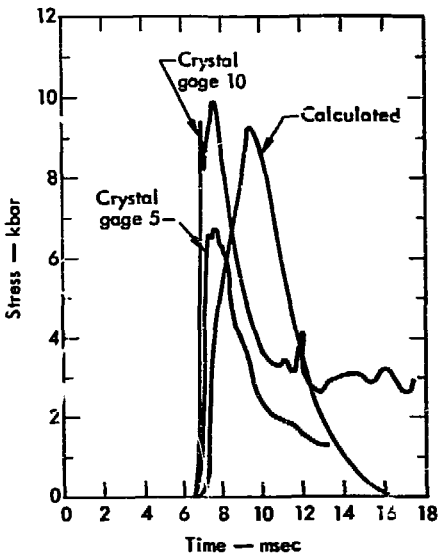

Fig. 12. Predicted and measured tangential stress at 45 m from shot.

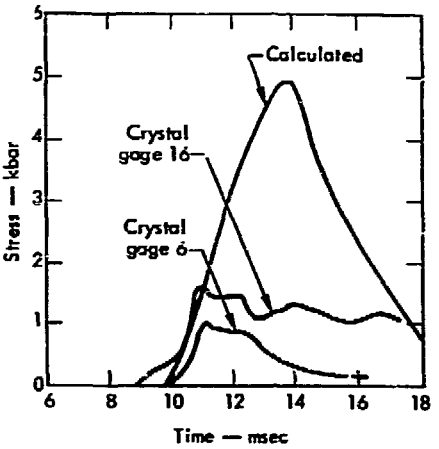

Fig. 13. Predicted and measured tangential stress at 63 m from shot.

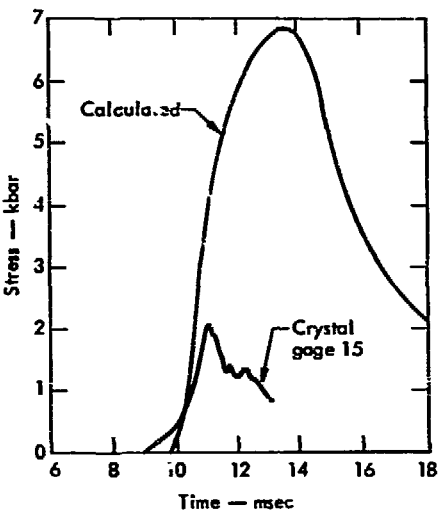

Fig. 14. Predicted and measured radial stress at 63 m from shot.

SEISMIC MEASUREMENTS

Roger G. Preston

Before the Handcar shot, it was considered that the seismic wave coupling would be similar to that in granite because dolomite's compressional velocities are about the same and it is a hard, albeit fractured, rock. The free-field seismic wave coupling in various media was determined by Werth and Herbst[7] (1963) from measurements in the elastic range in several media. Dan Patterson (LRL, private communication) has calculated the free-field peak particle velocities (Fig. 15) using the Werth-Herbst technique. Handcar free-field coupling was slightly better (20%) than tuff, but distinctly poorer than granite.

Data taken at sufficient distance to be sure the wave is elastic are the most significant. Measurements by LRL at Mina, Nevada (220 km), and Kanab, Utah (285 km), show that the Handcar displacement amplitudes are about one-sixth those of Hardhat, even though their shot locations are only 6.1 km apart. The Handcar amplitudes are about half of the average amplitudes from a shot in competent tuff (Blanca). Of course, suitable yield scaling has been done in deducing

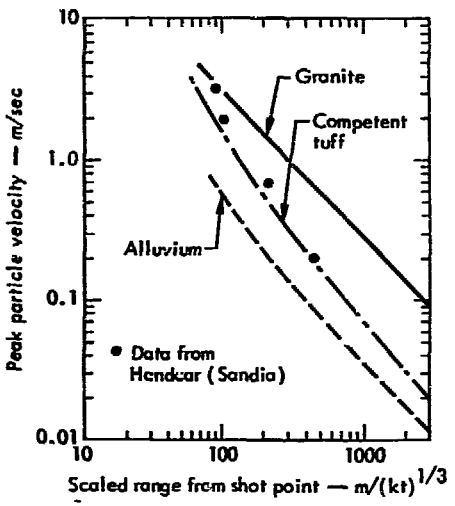

Fig. 15. Seismic coupling in Handcar dolomite compared with calculated coupling in alluvium, tuff, and granite.

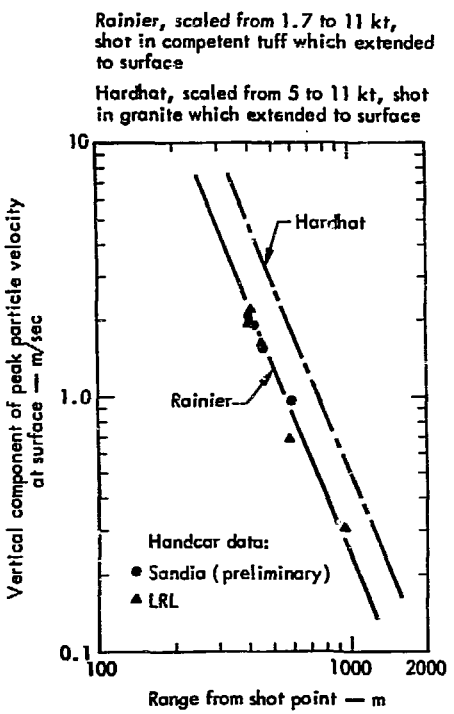

Fig. 16. Surface particle velocity vs distance from shot point. Scaled curves for Rainier and Hardhat compared to Handcar data.

these ratios. In considering these ratios, one should realize that distant seismic data scatter wildly (Don Springer, LRL, personal communication). We conclude that close in to the shot, free-field coupling is slightly better in dolomite than in competent tuff. When the highest frequencies are removed in the distant signal, free-field coupling in dolomite is about half that in competent tuff.

The surface measurements in the vicinity of surface zero are interesting because the shot was in hard rock overlain by softer alluvium. It is well known that when seismic waves couple from hard rock to soft rock, the amplitude of the particle velocity increases. With the seismic coupling of dolomite slightly greater than that of competent tuff, we find the experimental data over ground zero is about the same as that which would have been expected had it been tuff all the way to the surface (Fig. 16). This result is surprising and unexplained. The Rainier and Hardhat curves in Fig. 16 are taken from Sauer.[8]

CALCULATION OF DIFFERENCES BETWEEN ALLUVIUM AND HARD ROCK

William R. Hurdlow

Handcar was located in a unique geologic setting, with hard rock to the north and soft alluvium and tuff to the south. The geologic section is shown in Fig. 17. We are interested in determining if the TENSOR code can calculate the differences in amplitude between north and south directions caused by the change in the geologic section. The TENSOR code as used here propagates elastic waves through a Lagrangian mesh. The code has previously been described by Cherry and Hurdlow[9] (1966).

The abstraction of the Handcar cross section to the Lagrangian mesh calculation is shown in Fig. 18. The characteristic zone size is 50 m, which preserves 10 cps and below. Finer zoning would have preserved higher frequencies but would have required far more digital computing time. A 1-kbar seismic source step function was programmed in the region shown. Smoky Hill, 150 m high, has been preserved in the zoning. No attempt has been made to convolve an attenuation function or the actual source function as could be deduced from close-in measurements or from SOC calculations. The intent here is to get the relative effect of the hard rock to the north versus the alluvium to the south on the amplitude of the seismic wave.

The results of this calculation are shown in Fig. 19. The north and south results are similar. Smoky Hill causes no apparent effect. Wave amplitude is decaying less rapidly with distance through the alluvium to the south than through the hard rock to the north. The theoretical results have been normalized to the experimental data at 10 cm/sec. The seismic data are more variable to the north, where more topographic relief

exists, but at the more distant stations alluvium tends to have higher seismic-wave amplitudes. We have not attempted to incorporate the multiple spall mechanisms that occur directly over the shot into the TENSOR calculations.

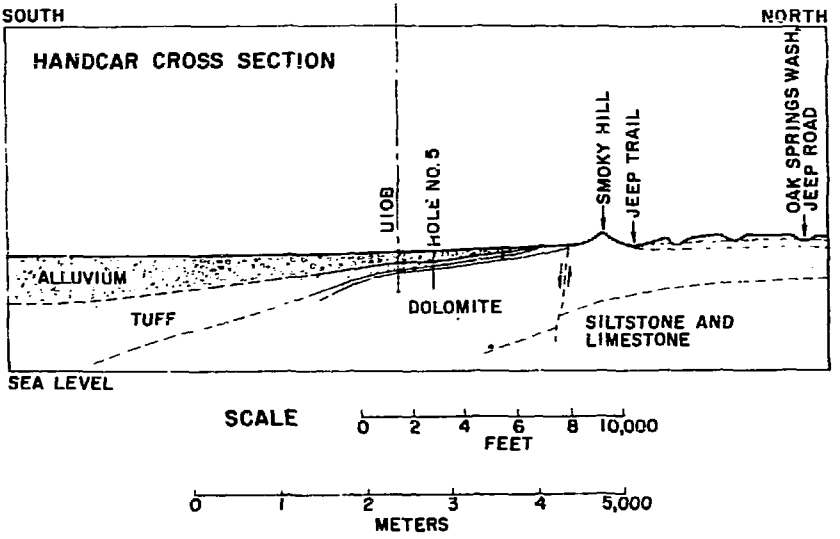

Fig. 17. North-south cross section through Handcar site, illustrating variations in geology.

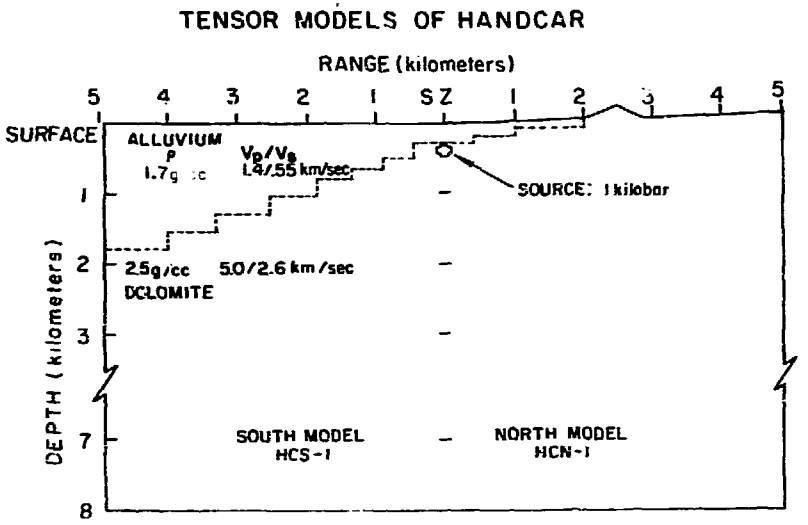

Fig. 18. Handcar geologic model used for calculations with TENSOR code.

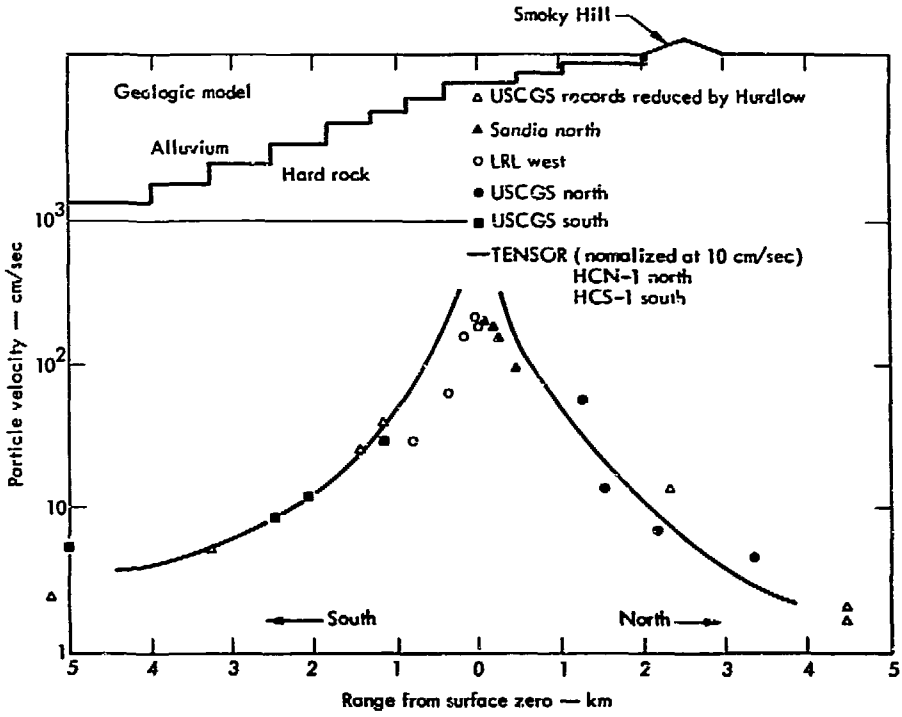

Fig. 19. Results of TENSOR calculation of Handcar seismic propagation.

Part II. Chemistry, Mineralogy, and Energy Distribution

R. W. Taylor

One of the goals of the Handcar experiment was to study chemical and mineralogical changes undergone by carbonate minerals as a result of a nuclear explosion.

This part of the report is a synthesis of chemical and mineralogical analyses of pre- and post-shot samples by F. Stephens, N. Smith, J. Kahn, and D. Emerson. In addition, radiochemical analyses of postshot solid and gas samples provided critical information on the extent of the chemical and mineralogical changes.

The changes in the rock caused by the thermal effects of the explosion are documented by contrasting the pre- and post-shot samples. We then deduce from these changes the specific conditions the samples experienced. It is important to point out that this can be done in much more detail for this explosion in dolomite

than for previous nuclear explosions which have been carried out, for the most part, in silicate rocks. The reason for this is that dolomite undergoes transitions that are distinct, well understood, heterogeneous, and first order. Furthermore, the principal transitions of dolomite liberate CO_2. The escape of CO_2 prevents reversal of the transition, leaving a telling record. Samples of gas taken after the explosion also document these transitions. The amount of gas liberated tells the amount of dolomite transformed, and thus the amount of energy required for these transformations can be calculated.

Silicate rocks, on the other hand, contain so many phases which undergo transitions of so diverse a nature that to unravel the chemical and thermal story of a nuclear explosion in silicates by examination of postshot debris is a much more difficult task. Even the melting of common silicate rock takes place over a wide temperature and energy range. Also, little gas is evolved except steam, which cannot be sampled effectively because it condenses.

PRESHOT CHEMICAL, MINERALOGICAL, AND TEXTURAL ANALYSES OF HANDCAR DOLOMITE

The chemical compositions of three composite samples of core from three depth intervals in the emplacement hole are given in Table 3. The composition is expressed both in terms of weight percent and mole percent. The samples are composed mostly (98.5-99.5%) of CO_2, CaO, and MgO. Notice the molar

Table 3. Chemical analysis of three preshot composite samples of Handcar core from hole U10b.[a]

	Sample from 1303-1346 ft		Sample from 1346-1373 ft		Sample from 1308.5-1373.9 ft	
Component	Wt %	Mole %	Wt %	Mole %	Wt %	Mole %
CO_2	46.48	48.98	46.82	49.31	46.18	48.76
CaO	30.63	25.33	31.02	25.64	30.96	25.65
MgO	21.07	24.23	21.24	24.42	21.21	24.44
SiO_2[b]	1.22	0.94	0.31	0.24	0.89	0.70
Al_2O_3[b]	0.48	0.22	0.25	0.11	0.40	0.18
Fe_2O_3	0.13	0.04	0.12	0.03	0.13	0.04
FeO	0.04	0.03	0.04	0.03	0.04	0.03
H_2O[c]	0.09	0.23	0.08	0.21	0.08	0.21
Totals	100.14	100.00	99.89	100.00	99.89	100.00

[a]Analyst, F. Stephens; first reported in a letter to M. Nordyke, Aug. 5, 1964.

[b]When these samples were placed in 6N HCl, the insoluble part consisted essentially of these amounts of SiO_2 and Al_2O_3 with traces of Fe, Mg, Ti, and other elements.

[c]Water lost at 155°C.

ratio, CaO/MgO = 1.048 ± 0.003. Also, notice that the number of moles of CO_2 is nearly equal to the sum of the number of moles of CaO and MgO. Thus the chemical composition of the rock is closely approximated by the formula

$$CaMg(CO_3)_2 .$$

The principal phase (mineral) in the Handcar rock was identified as dolomite by means of an x-ray diffraction* and optical study of 10 samples of preshot core from a zone near shot depth in hole U10b. The average weight percent dolomite in the zone of the Handcar explosion is 98.5 ± 0.5.

Microscopic examination of thin sections of these 10 samples of preshot rock gives a general idea of the variability in texture and grain size. This is also the best way of identifying minerals present in small amounts. Dolomite grains as large as 2 mm across are common, but the average size is about 0.2 mm. Calcite grains were also identified and in some cases they were twinned. Quartz (SiO_2), Fe_2O_3, and some clays were also identified, but they make up less than 2% of the rock. They constitute the acid-insoluble parts of the rock.

CHEMICAL AND MINERALOGICAL ANALYSES OF POSTSHOT SAMPLES

About a month after the Handcar explosion, a hole (U10b PS #1A Whipstock) was drilled into the area of the explosion. From this hole six of the 20 samples recovered were selected for analysis. The chemical composition of each of these samples, expressed in weight and mole percent, is given in Table 4. Because the hole from which these samples were taken was drilled using mud as a cooling fluid, the samples were all water-saturated. A total of 5000 m^3 of drilling mud was lost into the chimney.† This loss not only cooled the chimney but also probably caused the hydration of CaO (lime) and MgO (periclase) left after the thermal decomposition of dolomite.

Notice that these postshot samples, like the preshot samples, are made up mostly of CO_2, MgO, and CaO. The CaO/MgO mole ratio is 1.04 ± 0.02, probably not significantly different from the preshot value (1.048 ± 0.003).** In all cases these samples contain less CO_2 than the preshot samples. This is taken as evidence of thermal decomposition of dolomite, the details and implications of which are discussed in the next section. The extent of decomposition of the six

*The ASTM-tabulated d-spacings for reflections from the planes (404) and (318) in dolomite are 1.0074 Å and 1.0002 Å, respectively. The corresponding spacings in Handcar dolomite are 1.007_3 Å and 1.000_2 Å.

†To boil this much water would require 4 kt of energy, one-third of the total energy of the Handcar explosive.

**The solubility of CaO in water, producing $Ca(OH)_2$, is 0.1 g/100 ml; the solubility of MgO, producing $Mg(OH)_2$, is ~0.001 g/100 ml at ~40°C; thus CaO could have been leached by the drilling mud.

Table 4. Chemical analysis of six Handcar postshot samples.[a]

Sample depth[b] (ft)	1455		1452		1407		1464		1444		1427	
Basis	Wt %	Mole %	Wt %	Mole %	Wt %	Mole %	Wt %	Mole %	Wt %	Mole %	Wt %	Mole %
CO_2	32.96	45.68	2.43	4.20	44.96	47.82	37.03	47.99	42.73	45.93	44.14	47.12
CaO	35.72	30.34	36.30	32.05	30.01	25.03	32.74	27.65	30.19	25.65	30.26	25.45
MgO	25.14	29.70	36.45	39.98	20.71	24.03	24.11	27.14	20.88	24.67	20.59	23.99
SiO_2	4.42	4.52	4.14	3.79	3.23	2.52	3.30	2.60	3.65	2.90	3.65	2.85
Al_2O_3	1.29	0.66	0.46	0.25	1.00	0.46	1.10	0.51	1.53	0.71	1.15	0.53
Fe_2O_3	0.53	0.16	0.45	0.13	0.30	0.09	0.26	0.08	0.40	0.12	0.33	0.10
FeO	0.01$_5$	0.00$_5$	0.04	0.03	0.08	0.05	0.07	0.04	0.06	0.04	0.09	0.06
Totals	100.08	100.00	99.87	100.00	100.32	100.00	99.62	100.00	99.22	100.00	100.21	100.00
Insoluble (wt %)	5.60		4.40		4.7		4.90		6.80		5.40	

[a]Chemical analysis of six postshot samples by N. Smith, LRL, Feb. 9, 1965.

[b]Distance down Hole PS #13 Whipstock from which sample was recovered. Shot point depth (1320 ft) measured down this slanted hole is at 1401 ft.

postshot samples can be measured by the amount of CO_2 they have lost. That is, 100 g of typical Handcar rock losing the amount of CO_2 given in Table 5 will have approximately the observed postshot composition. The reason this measurement is approximate is that the postshot samples contain about three times as much acid-insoluble components (4.9 to 6.8 wt%) as the preshot rock. The principal component of the insoluble fraction is SiO_2, as it was in the preshot samples. The Si/Fe ratio in the postshot samples is about twice that in the preshot samples. The increased amount of insoluble (noncarbonate) material in the samples taken after the explosion probably came from the high-silica grout used to emplace the explosive. The increased amount of iron probably came from the iron well casing and from iron in the explosive canister.

The Fe_2O_3/FeO mole ratio in the preshot rock is about 1. The postshot samples are considerably oxidized, having Fe_2O_3/FeO ratios of about 2 and greater. This is surprising because the introduction of metallic iron into the system at high temperatures would be expected to result in an Fe_2O_3/FeO ratio between 1/2 and 1. Also, in equilibrium with CO_2, the Fe_2O_3/FeO ratio is expected to be about 1. The oxidation of the postshot samples was probably caused by

Table 5. Weight percent CO_2 lost by Handcar postshot samples.

Sample type	Sample depth (ft)	Grams CO_2 lost per 100 g preshot rock[a]
Chimney	1407	2.7
	1427	4.2
	1444	7.0
Diagnostic[b]	1452	24.3
	1455	20.2
	1464	12.2

[a]Based on an average preshot rock containing 46.49 g CO_2 per 100 g of rock (Table 3), and calculated by the approximate formula

$$Y_2 \approx Y + \frac{\phi X}{(\phi - 100)}$$

where

Y_2 = wt% CO_2 lost,

Y = wt% CO_2 in preshot rock (46.49%),

X = wt% non-CO_2 in preshot rock (100 - Y) = 53.51,

ϕ = measured wt% CO_2 in postshot samples.

[b]Samples from "puddle glass" at bottom of cavity.

steam when water was introduced during the postshot drilling. This indicates that the rock was still hot enough to generate steam, although the maximum postshot temperature measured was only 50°C.

Examination of these six postshot samples by x-ray diffraction showed dolomite, calcite, and MgO (periclase). The sample from 1452 ft was the only one in which CaO (lime) was identified. Notice that this is the sample which contains the least CO_2, having lost about 24 g of CO_2 per 100 g of preshot rock. As will be discussed in more detail later, dolomite decomposes upon heating by a two-stage loss of CO_2. The first stage results in the formation of $CaCO_3$ (calcite) and MgO. The second stage, at higher temperatures, results in the decomposition of $CaCO_3$ to form CaO and CO_2. Thus, it is not surprising that the sample of postshot rock which lost the most CO_2 is the one in which lime was found as a distinct phase.

Examination of thin sections of these six postshot samples revealed a great textural variation. The largest grain size is found in samples from the shallowest depths, 1407 and 1427 ft. These are the two samples closest in chemical composition and mineralogy to the preshot rock. Even these samples, however, show optical as well as chemical evidence of some thermal alteration. They contain less CO_2 and more calcite than the average preshot rock. In addition, they contain some periclase (MgO) which was not found before the shot.

Samples from 1452 and 1455 ft do not look at all like the original rock. The grains are rounded, involuted, and embayed. These samples probably represent a nearly completely decomposed rock. Other samples show intermediate stages of decomposition. In some cases nearly unaltered dolomite is mixed with very altered material. Slip across a twinned grain of calcite is evidence of deformation. The mineralogical composition as deduced from chemical analysis is in agreement with the observed mineralogy as shown in Table 6.

The most difficult textural feature to explain is what appears to be melting. The "melting" is confined to occasional grain boundaries in samples from 1407 and 1427 ft, which are relatively unaltered. Other samples show what looks like melted rock surrounding most grains. Both calcite and dolomite melt at temperatures above about 1400°C, but only at a CO_2 pressure greater than 80 atm in the case of calcite and greater than 10,000 atm in the case of dolomite. Any textural evidence of the melting of these carbonates would be destroyed by subsequent decomposition as the CO_2 pressure fell. Furthermore, if any of these six postshot samples had been heated above 1200°C, the quartz grains in them would have been converted to either a high temperature modification of SiO_2 such as cristobalite or to silica glass. This clearly did not occur, since quartz was found in the acid-insoluble fractions of the postshot samples. Thus it seems that the rounding of grains and other textures were not caused by partial melting. Probably CaO and MgO, formed on the edges of carbonate grains, reacted with water and steam introduced

during drilling to form hydroxides, which look like a liquid. Conditions to form hydroxides are not inconsistent with the conditions postulated earlier in this section of the report to explain the oxidation of iron in the postshot samples.

Table 6. Mineralogical analysis of six Handcar postshot samples.

	Chimney samples						Diagnostic samples[a]					
	1407 ft		1427 ft		1444 ft		1452 ft		1455 ft		1464 ft	
Mineral	Calc.[b]	Obs.[c]	Calc.	Obs.	Calc.	Obs.	Calc.	Obs.	Calc.	Obs.	Calc.	Obs.
Dolomite	89.6	1	85.3	1	79.2	1	0	3	20.7	2	56.1	1
Calcite	4.8	2	7.6	2	11.1	—	66.7	1	52.5	1	28.2	1
Periclase	1.1	—	1.9	—	3.6	—	26.7	2	20.6	—	10.9	—
Lime	0	—	0	—	0	—	0.9	—	0	—	0	—
SiO_2	3.2	—	3.6	—	4.1	—	4.1	—	4.4	—	3.3	—
Other	1.4	—	1.6	—	2.9	—	1.5	—	1.8	—	1.4	—

[a]Samples from "puddle glass" at bottom of cavity.

[b]Calculated mineralogical composition in weight percent, based on the knowledge that calcite is more stable than dolomite which is more stable than magnesite ($MgCO_3$).

[c]In order of abundance, as determined from microscopic observation and x-ray study.

CHARACTERIZING THE THERMAL DECOMPOSITION OF DOLOMITE

The subject of the previous section was the chemical and mineralogical changes in the Handcar dolomite rock caused by a nuclear explosion. To determine what conditions were necessary to cause the observed changes, we must understand the thermal decomposition of dolomite. In order to gain insight into the way energy is deposited by a nuclear explosion we also need to review what is known about the amount of energy required to heat and decompose dolomite. Knowing how much energy is required to bring dolomite to some stage of decomposition and how much dolomite was decomposed to that stage, we can conclude what fraction of the total energy was taken for that process. In the next section we will consider these ideas in more detail, presenting data on the amount of dolomite decomposed, as deduced from gas samples and from the fraction of the total radioactivity a given postshot sample contains.

Perhaps the most familiar way of representing the decomposition of a carbonate is a plot of the CO_2 pressure as a function of temperature. Such plots for dolomite and its components, calcite and magnesite ($MgCO_3$), are given in Fig. 20. This figure is complicated considerably because it includes the CO_2 pressures for the invariant equilibria of coexisting pairs of these carbonates.

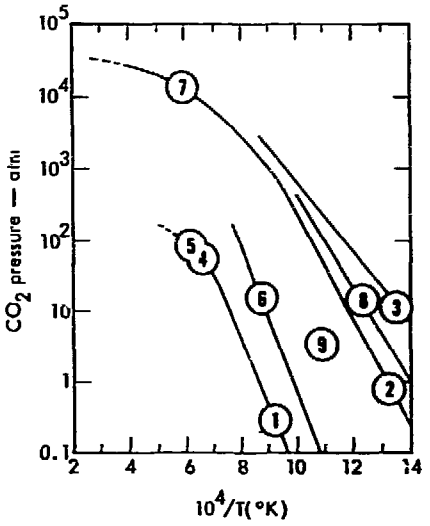

Fig. 20. Carbon dioxide pressure vs temperature for the system $CaCO_3$-$MgCO_3$. Key to the various curves and areas is: 1. $CaCO_{3(s)} = CaO_{(s)} + CO_{2(g)}$. 2. $MgCa(CO_3)_{2(s)} = MgO_{(s)} + CaCO_{3(s)} + CO_{2(g)}$. 3. $MgCO_{3(s)} = MgO_{(s)} + CO_{2(g)}$. 4. At T = 1520°C, $CaCO_3$ = liquid + $CO_{2(g)}$. 5. Melting point of $CaCO_3$. 6. CO_2 pressure for coexistence of calcite ss (solid solution) and dolomite ss. 7. Melting point of dolomite. 8. Coexistence of dolomite ss and magnesite ss. 9. Conditions for stability of dolomite ss extend from curve 6 to curve 8.

Such a representation of data (Fig. 20) is incomplete and confusing unless one understands that these carbonates are solid solutions. The CO_2 pressure for a solution at any temperature depends upon the composition of the solution. This is illustrated in Fig. 21, in which carbonate composition and temperature are the coordinates. The equilibrium CO_2 pressure for any composition and temperature is given by the dashed lines. These figures are based on a large amount of experimental data.[10-15] The solid lines are phase boundary curves. These lines separate areas of one condensed phase (solid or liquid) from areas of two condensed phases. Notice, particularly, that dolomite is a solid solution of $CaCO_3$ and $MgCO_3$. At temperatures above about 1000°K the compositional range for dolomite expands rapidly, and above 1400°K the distinction between dolomite and calcite disappears.

To use Fig. 21 one may find, for example, what CO_2 pressure would result when a rock composed mostly of dolomite and calcite is heated to 1200°K. Look in the phase area, labeled calcite and dolomite, and find that the CO_2 pressure is about 50 atm.

Under these conditions, if the pressure falls below 50 atm at 1200°K, Fig. 21 does not indicate what happens. This is best illustrated in another kind of diagram, shown in the next five figures (Figs. 22-26). These figures are isothermal

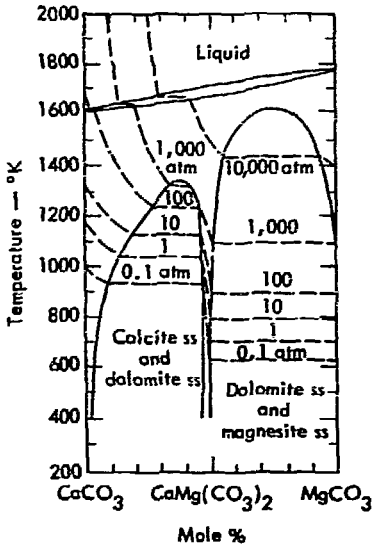

Fig. 21. Phase equilibria in the system $CaCO_3$-$MgCO_3$, showing CO_2 pressure.

sections through the compositional prism, the corners of which are CaO, MgO, and CO_2. Under the conditions of temperature and pressure illustrated here, the decomposition of dolomite can be described in terms of a three-component or ternary system.

First, let us examine Fig. 22. For purposes of understanding the chemical and mineralogical changes observed in the postshot Handcar samples, let us imagine a line a-a' drawn for Ca/Mg = 1 (atom ratio). This line goes through the composition $CaMg(CO_3)_2$ (dolomite). The compositions of the six postshot samples lie along this line as shown. Compositions along this line, down from the point representing dolomite, represent an increasing loss of CO_2. Notice that the postshot sample from 1452 ft having lost the most CO_2 is plotted the greatest distance from the point representing dolomite—in a direction away from CO_2. From Table 4 one can easily recalculate the composition of the sample from 1452 ft in terms of these three components as 33.1 mole % CO_2, 34.0 mole % CaO, and 32.9 mole % MgO.

In Fig. 23, the phase boundaries for this ternary system are indicated. In Figs. 24-26, approximate phase relations are shown for progressively higher temperatures. Notice that the three-phase areas decrease in size and the two-phase areas increase in size with increasing temperature until at about 2000°K most of the lower half of the phase diagram is dominated by a single liquid phase. For a given composition an increase in temperature results in an increase in CO_2 pressure.

The useful application of these diagrams for the present problem is to follow the decomposition of dolomite with increasing temperature at a fixed CO_2 pressure. It is not unreasonable to assume that the CO_2 pressure in the cavity created by the Handcar explosion was at lithostatic pressure (~80 atm) for some time. Certainly it could not have been at a pressure more than this for long, nor could the CO_2 pressure have been less than 1 atm. Thus, any dolomite heated as hot as 1000°K at a CO_2 pressure of 80 atm would not have decomposed at all. If, at the same temperature, the CO_2 pressure were 1 atm, CO_2 would be lost by dolomite and the bulk composition of the remaining condensed phases is described by the line a-a'. The extent of decomposition at 1 atm is given by the intersection of line a-a' and the three-phase field where

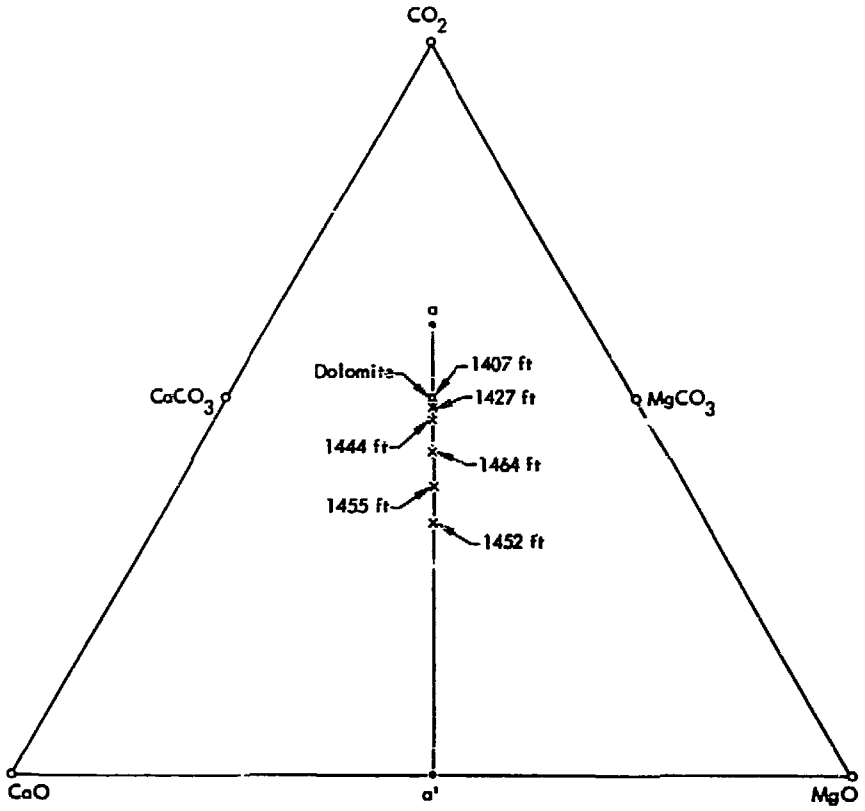

Fig. 22. Composition of six Handcar postshot samples expressed in terms of their principal components, CaO, MgO, and CO_2.

the CO_2 pressure is thought to be about 1 atm. That is precisely the composition where CaO first forms. Notice that at equilibrium, no dolomite would remain and the final assemblage would consist of approximately equal amounts of MgO and $CaCO_3$. The situation at 1300°K is similar, but at a CO_2 pressure of 80 atm dolomite decomposes into MgO and $CaCO_3$. At 1300°K and 1 atm, dolomite is completely decomposed into a mixture of CaO and MgO. At 1600°K dolomite is completely decomposed unless the CO_2 pressure is greater than about 5 kbar. At about this temperature a mixture of CaO and $CaCO_3$ will melt at a CO_2 pressure of about 90 atm. At 2000°K, most compositions in the system form carbonate liquids, but at CO_2 pressures too high to be the cause of the textures which resemble melted rock seen in all six postshot samples (as discussed in the previous section).

Figure 27 was prepared to summarize the thermal decomposition of dolomite at a CO_2 pressure of about 100 atm.

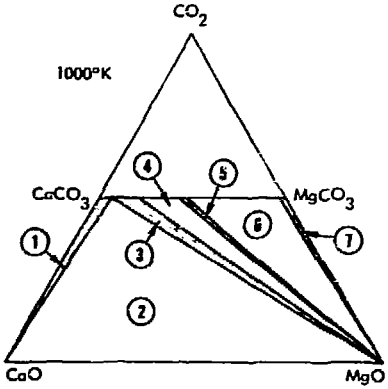

Fig. 23.

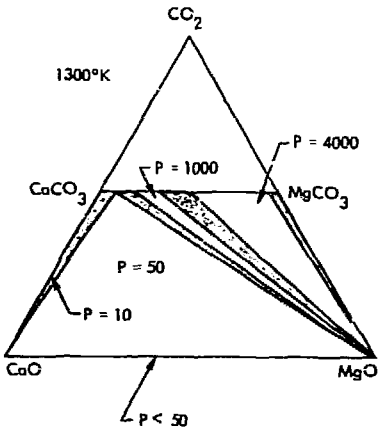

Fig. 24

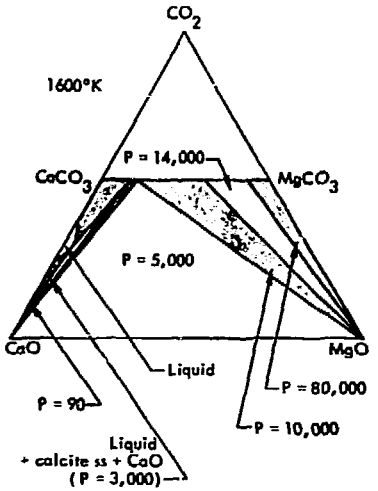

Fig. 25

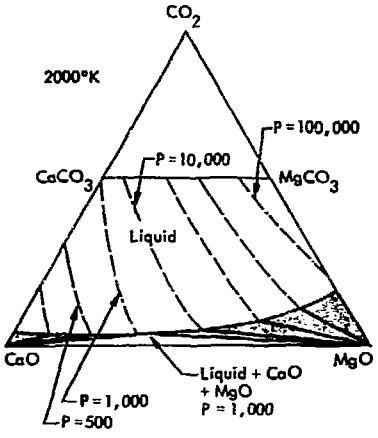

Fig. 26

Figs. 23-26. Phase boundaries for the ternary system CaO-MgO-CO_2. Lower half of Fig. 23 is divided into seven areas. From left to right, the areas are:

1. A two-phase area where calcite ss (solid solution) and CaO exist together at equilibrium. CO_2 pressure 0.1 atm.
2. A three-phase area (calcite ss of fixed composition, CaO, and MgO) with a fixed CO_2 pressure of 1 atm.
3. A two-phase area of coexisting calcite ss and MgO.
4. A three-phase area of calcite ss, dolomite ss, and MgO coexisting at a CO_2 pressure of about 50 atm.
5. A two-phase area of dolomite ss and MgO.
6. A three-phase area of coexisting dolomite ss, magnesite ss, and MgO at a CO_2 pressure of about 750 atm.
7. A two-phase area of magnesite ss and MgO at CO_2 pressures between 750 and 1000 atm.

Figures 24-26 show the change in phase boundaries at progressively higher temperatures.

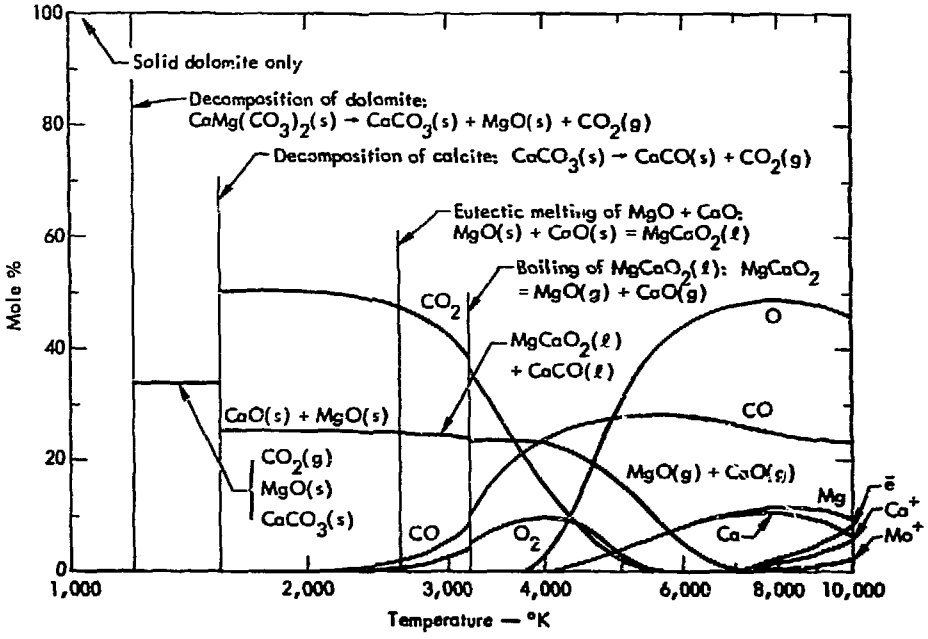

Fig. 27. Thermal decomposition of dolomite at CO_2 pressure of 100 atm.

Here, the molecular composition of dolomite is plotted as a function of temperature. Above about 3200°K, the system becomes a single gas phase. Data on the thermal dissociation of gaseous MgO, CO_2, and O_2 was taken from the literature.[16-20] For lack of data, vaporization of liquid CaO was assumed to take place at the same temperature as vaporization of MgO. Thermal ionization was calculated like thermal dissociation where the ionization potential is related to the dissociation energy in a way suggested by Saha and Srivastava.[21]

Figures 24-27 illustrate that CaO and MgO, free of CO_2, form from dolomite at temperatures above ~1000°K at a CO_2 pressure of 1 atm, or at temperatures above ~1300°K when the CO_2 pressure is less than 50 atm. Thus, it was expected that quantities of these oxides would be found in the postshot debris, including some 2000 tons or so of melted oxides (mixtures of MgO and CaO melt at ~2600°K). As it turned out, no postshot sample was free of carbonate, and no sample showed clear evidence of having been heated above about 1200°K.

One must bear in mind that back reactions between the oxides CaO and MgO with CO_2 to form carbonates can, in principle, take place upon cooling in a fixed CO_2 pressure. Can this be the

source of carbonate in some of the postshot samples? From the data just presented, the temperatures below which MgO and CaO can react with a given CO_2 pressure to form carbonates can be determined. Notice that $CaCO_3$, calcite, is favored. That is, at a given CO_2 pressure CaO can react to form $CaCO_3$ at temperatures more than 500° higher than MgO can. For example, under a CO_2 pressure of 1 atm, CaO reacts to form $CaCO_3$ when the temperature falls to 1150°K. Periclase (MgO) reacts to form $MgCO_3$ only when the temperature falls to ~640°K. This is too low a temperature to expect rapid reaction to take place.

In order to reform dolomite, which is $CaMg(CO_3)_2$, from its constituent carbonates, reaction between two solids involving diffusion in the solid state is required. This probably did not take place to any significant extent following the Handcar explosion. Back reaction of CaO with CO_2, on the other hand, is known to be rapid at 1000°K, at least until a surface layer of carbonate about 1 mm thick forms. This is probably thicker than the CaO particles left after the decomposition of dolomite. Thus, solid MgO and $CaCO_3$ should be expected in postshot debris that is cooled in CO_2.

Experimental data are needed on the rate of these reactions. Probably the most important factor determining the amount of $CaCO_3$ which forms by back reaction is the collapse of the cavity. When this happens the CO_2 is displaced upward by falling rock and is thus removed from the hot solid CaO and MgO with which it might otherwise have reacted. The Handcar chimney collapsed within 35 sec after detonation.

AMOUNT OF DOLOMITE DECOMPOSED, AS ESTIMATED FROM GAS AND SOLID SAMPLES

From the practical point of view, it is important to know the amount of CO_2 generated by a nuclear explosion in carbonate-bearing rock in order to prevent the escape of radioactive gases. Also, if the total amount of CO_2 generated is known, then the total amount of energy required for this process can be calculated. If this fraction of the total energy yield is independent of the total yield, it may be possible to measure the energy release of a nuclear explosion from the amount of CO_2 released.

In Part III of this report the results of the radiochemical studies are presented and discussed. It is shown that about 4×10^7 moles of CO_2 was evolved. This value is the average of the results calculated by several methods based on ^{85}Kr and ^{14}C. It appears that the tracer gases were not well mixed. This was probably due to the generation of CO_2 free of tracer from the thermal decomposition of dolomite for several hours after the explosion. This CO_2 displaced radioactive gases out of the chimney as far as 170 m into the surrounding rock so that gases sampled from the chimney region were not as radioactive as a true average sample would have been.

The amount of dolomite decomposed to release 4×10^7 moles of CO_2 is

2×10^7 moles, or 3.7×10^9 g. This corresponds to about 310 metric tons of dolomite per kt of yield (based on 12 kt total yield).

Another way of estimating the total amount of CO_2 evolved comes from the radiochemical examination of solid postshot samples selected from depths where maximum radioactivity was detected. Each Handcar sample was examined for various radioactive elements. The fraction of the total of a given radionuclide found in a sample tells how large such a sample would have to be to contain all of the radioactivity.

It seems reasonable to combine the information on the amount of thermal decomposition in each postshot sample with the information on the amount of other similar material that can exist, the reciprocal device fraction. In general, the closer a sample was to the explosion, the hotter it was heated, the more CO_2 it could have lost, and the more radioactivity it could have picked up. The relevant data are given in Table 7. Although the data show considerable scatter, the trend is clear and in agreement with expectations. The total amount of CO_2 generated as estimated by this

Table 7. Amount of CO_2 released, based on solid postshot samples.

Sample depth (ft)	CO_2 lost, Δ[a] (wt%)	Log Δ	Reciprocal of "bomb fraction," ϕ[b] (10^{11} g)	Log ϕ	Total CO_2 generated (10^9 g)	Total CO_2 generated (10^7 moles)
1407[c]	2.7	0.431	3.01	11.48	6.0	14.0
1427[c]	4.2	0.623	5.55	11.74	23.0	52.0
1444[c]	7.0	0.845	1.05	11.02	7.3	17.0
1452[d]	24.3	1.38	0.0265	9.42	0.64	1.4
1455[d]	20.2	1.30	0.0777	9.89	1.6	3.6
1464[d]	12.2	1.09	0.0942	9.97	1.1	2.5
				Overall average	6.6	15.0
				Diagnostic sample average	1.1	2.5

[a] From Table 5.

[b] The amount of material one would have if the sample were enlarged, maintaining its same percentage composition, until it contained all the refractory radioactive elements produced in the explosion.

[c] Chimney samples.

[d] Diagnostic samples, from puddle glass.

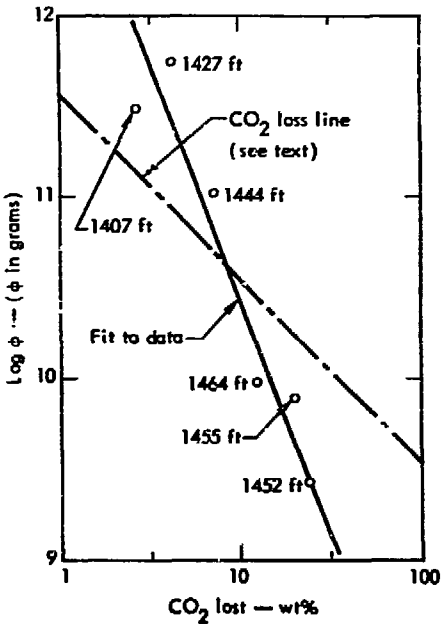

Fig. 28. Log of reciprocal bomb fraction, ϕ, vs CO_2 lost.

method is 1.5×10^8 moles, four times as much as the estimate based on ^{85}Kr and ^{14}C dilution. If only those samples considered of diagnostic quality are considered, the total CO_2 estimate, 2.5×10^7 moles, is in better agreement with the estimate based on the gas samples.

Figure 28 shows the relation between the decomposition of samples caused by heat from the explosion and the concentration of refractory radioactive elements from the explosion. It appears that the upper three samples, the chimney samples, have undergone thermal decomposition without picking up much radioactivity compared to the lower three samples. The dot-dashed line across Fig. 28 represents the relation between the amount of CO_2 released per gram and total number of grams losing this amount of CO_2 so that the total loss of CO_2 is 4×10^7 moles.

AMOUNT OF ENERGY INVOLVED IN HEATING AND DECOMPOSING DOLOMITE, AND A COMPARISON WITH OTHER EXPERIMENTS

The enthalpy necessary to heat and decompose dolomite is given in Fig. 29.[16-21] Estimates of the total amount of dolomite decomposed were made in the previous section. In this section these data are combined in order to estimate the total amount of energy involved in decomposing dolomite.

From Fig. 29 it can be seen that about 300 cal/g is needed to heat and decompose dolomite into $CaCO_3$, MgO, and CO_2. To decompose dolomite into CaO, MgO, and $2CO_2$ requires about 600 cal/g. Thus, the amount of energy per mole of CO_2 is the same for either the low- or high-temperature decomposition of dolomite. The value is ~55 kcal per mole of CO_2. Taking 4×10^7 moles of CO_2 as an estimate of the total amount of CO_2 released by the explosion, we find that the total amount of energy used in decomposing dolomite was 2.7×10^{12} cal. This is 2.7 kt or about 22% of the total amount of energy liberated in the explosion.

There have been five other underground nuclear explosions studied in sufficient detail to make estimates of the amount of rock receiving sufficient thermal energy to cause a recognizable change. In the Gnome and Salmon explosions, 970

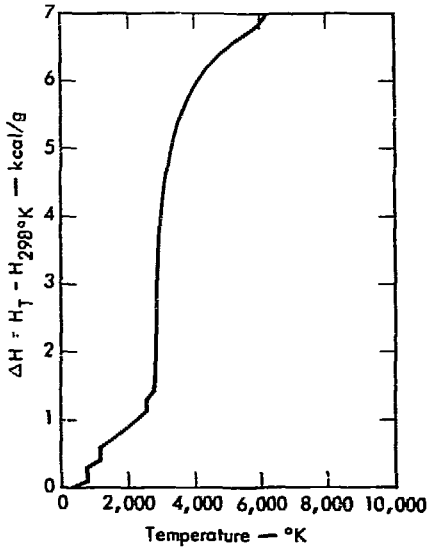

Fig. 29. Enthalpy curve for heating and decomposing dolomite.

± 100 tons of salt was melted per kiloton of yield. It takes 300 cal/g to heat and melt salt. For both of these experiments about 30% of the total energy released was required to melt salt.

In the Rainier and Hardhat experiments, 700 ± 100 tons of silicate was melted per kiloton of yield. It requires about 500 cal/g to melt silicates. The total fraction of the yield involved in melting silicates was about 37%.

The Gasbuggy experiment was a 29 ± 3 kt explosion in shale. The shale contained 10^{-3} mole of CO_2 per gram, mostly as dolomite. Gas samples taken after the explosion indicate 4.22×10^7 moles of CO_2 was liberated from the rock. The total amount of energy required to produce the observed amount of CO_2 for the Gasbuggy experiment was about 16.7 kt or 57% of the total energy of the explosion.[22]

It is important to understand why twice as much energy was involved in thermal alterations of rock at temperatures above 900°K in the Gasbuggy experiment as in the Handcar and other previous experiments. Our estimates of the amount of CO_2 expected in the Gasbuggy chimney were low by a factor of 2 because they were based on Handcar and other earlier experiments. Factors which play a role in the fraction of the total energy involved in heating rock to various temperatures (energy fractionation) have not been investigated. It is easy to suspect that yield, as well as water content and permeability, plays a major role in energy fractionation. Gasbuggy was about three times the yield of Hardhat and Handcar, and about six times the yield of Rainier, Gnome, and Salmon. For one thing, the greater the yield, the deeper will be the puddle of molten rock. The time necessary for cooling a puddle increases with the size of the puddle, other factors being equal.

If yield is important to the energy disposition we should examine very large yield experiments for unusual thermal effects. For example, the bomb fractions per volume of postshot gas samples may be smaller than usual (e.g., the maximum values observed for large explosions may be 10 times smaller than the maximum values for smaller explosions). Such a large decrease is not expected in the case of solid postshot puddle samples because the excess rock melted by the large yield explosion is probably not well mixed with the shock-melted rock containing most of the refractory radioactive elements.

Part III. Distribution of Radioactive Debris in the Handcar Chimney

C. F. Smith

One important aspect of the experimental program for Handcar was the investigation of the distribution of certain radioactive nuclides in the postshot nuclear chimney. These investigations were designed to evaluate the effects of the carbonate medium on gas composition, both chemical and radiochemical, and on the distribution of nonvolatile debris between chimney and "puddle glass" regions. On the following pages the unclassified parts of these efforts are discussed in some detail. The classified work is discussed in UCRL-50967.

The results reported here represent the efforts of a large number of workers. Descriptions of the various topics came originally from the program chairmen acknowledged in the section headings. The descriptive text has been edited and supplemented to some extent to reflect the improved understanding of some of the phenomena which has been gained since the original writing, and for the sake of completeness.

RADIOACTIVITY

W. E. Nervik

An important objective of the Handcar experiment was to determine the postshot distribution of radioactive debris from nuclear devices exploded in a carbonate medium. To measure this distribution for the nonvolatile debris, plans were made to drill two postshot sampling holes through the subsurface rubble zone as soon after zero time as was safe and practical. A sufficient number of core samples from these holes were to be chosen to provide a reasonable mapping of the total rubble volume and were to be analyzed for about 12 radioactive species.

As it turned out, only one useful postshot hole was drilled. Twenty core samples were obtained from this hole, but through a combination of events, including labor and equipment shortages and drilling difficulties caused by the dolomite medium, analysis did not begin until H + 2 months, so isotopes with half-lives less than 7 days or so could not be measured.

A cross section of the postshot chimney one year after the detonation of Handcar is presented in Fig. 30. Twenty sidewall samples were obtained from the U10b PS #1A Whipstock reentry hole at depths roughly indicated by the solid dots in Fig. 30 (Ref. 4). Data presented here were obtained by analysis of the most active seven of the 20 samples recovered. Sample numbers correspond to the order of analysis.

Based on analysis of debris from a large number of underground nuclear

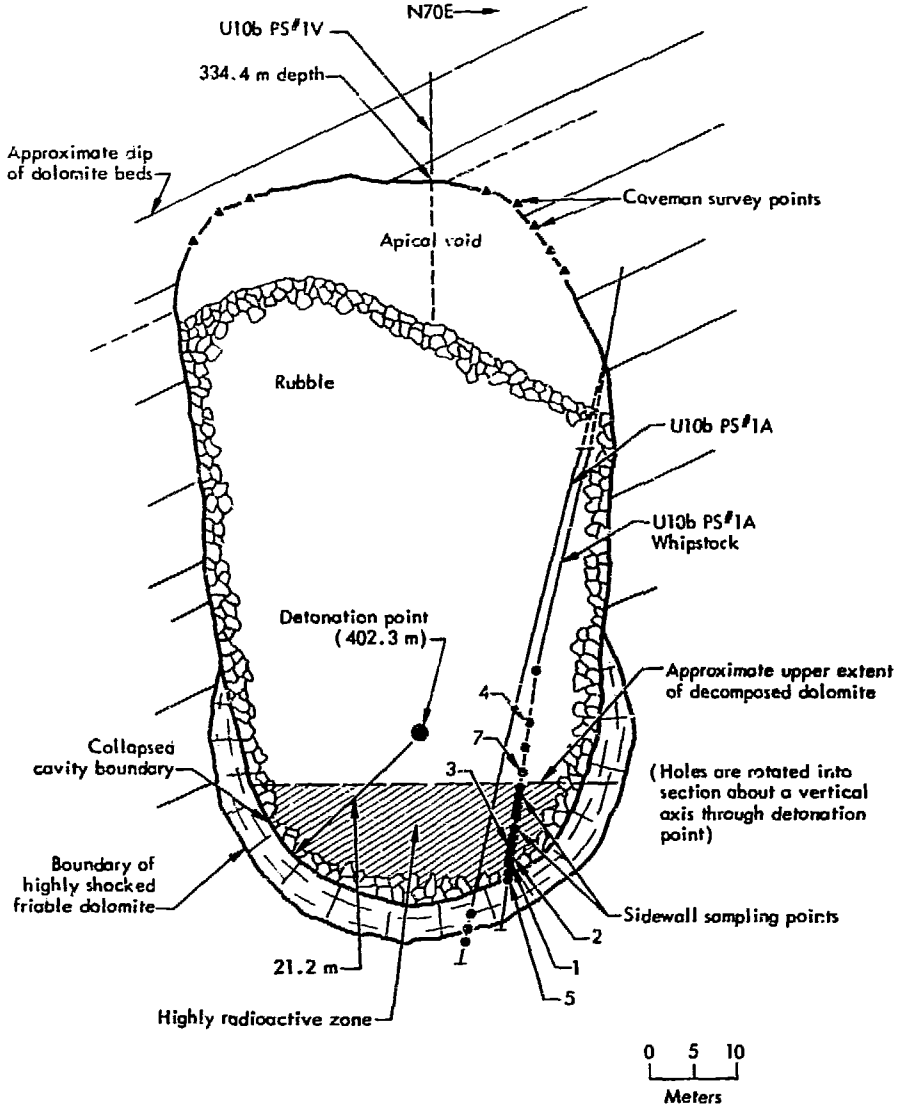

Fig. 30. Vertical section through Handcar chimney 1 yr after the explosion.

detonations, the following sequence of events is believed to take place:

When the explosion occurs, the walls of the growing cavity are lined with a

thin layer of melted rock which remains relatively intact when the cavity subsequently collapses. This melt retains the refractory elements while the volatile elements are distilled off and condense in the chimney rubble above. Samples of the cooled melt (diagnostic or puddle samples) and samples of the chimney rubble (chimney samples) are obtained from the postshot drilling operation. The fission yield of a device is measured by the ratio of the amount of a fission product to the amount of fissionable material (or a material added as tracer for the fissionable material) measured in a given sample. The best measure of the yield should be obtained from ratios of refractory materials retained in the melt, since these materials distill only a very small fraction of their total amount into the chimney region.

For example, if material X lost a fraction α by distillation, and material Y lost a fraction β by distillation, then the ratios of the amounts of X and Y are:

$$\frac{(1-\alpha)X}{(1-\beta)Y} = \frac{X'}{Y'} \quad \text{(puddle sample)},$$

$$\frac{\alpha X}{\beta Y} = \frac{X''}{Y''} \quad \text{(chimney sample)},$$

where X and Y represent total amounts of each in the system.

If α and β are small then the measured ratio X'/Y' in the puddle is very close to the true value X/Y, whereas the ratio X"/Y" in the chimney is probably not equal to X/Y and we have no way of measuring α/β to calculate X/Y. Chimney samples are therefore of little diagnostic value. If α is large and β is small (X volatile, Y refractory), then X'/Y' in the puddle will be low and X"/Y" in the chimney will be high. The true values of X/Y for a number of fission products are known from calibration experiments and are reported as R-values.* Some of these fission products are refractory (^{147}Nd, ^{144}Ce, ^{156}Eu) and some have volatile members in the decay chain (^{89}Sr, ^{90}Sr, ^{91}Y, ^{127}Sb, ^{132}Te, ^{131}I, ^{140}Ba, and ^{141}Ce). R-values for this latter group should be lower than expected for diagnostic samples and higher than expected for chimney samples, providing a positive means of identification of the more significant diagnostic samples.

Table 8 summarizes the fission product data for the Handcar samples. Pots 1, 2, 3, and 5 are diagnostic samples. Pots 4, 6, and 7 are chimney samples. Chemical and mineralogical analyses of six of these samples are given in Tables 4-6 of the previous section of this report.

Note in Fig. 30 that with the possible exception of pot 6, this grouping into diagnostic and chimney samples is dependent on sampling depth, although it may be fortuitous. Within these groups no such trend in R-values as a function of depth is observed. As discussed in

*A fission product R-value of mass A is defined as follows:

$$R(A) = \frac{\frac{C(A)}{C(99)_{meas}}}{\frac{C(A)}{C(99)_{std}}} \Big/ \frac{\frac{Y(A)}{Y(99)_{meas}}}{\frac{Y(A)}{Y(99)_{std}}}$$

where
$C(A)$ = counting rate of isotope of mass A,
$C(99)$ = counting rate of ^{99}Mo,
$Y(A)$ = fission yield of isotope of mass A,
$Y(99)$ = fission yield of ^{99}Mo,
$(\ )_{meas}$ = experimental conditions,
$(\ )_{std}$ = ^{235}U + thermal neutrons.

Table 8. Fission product R-values for the Handcar samples.

Nuclide	Unfractionated R-value	Maximum diagnostic sample R-value	Pot 1 Sampling depth (ft) 1455	Pot 2 1452	Pot 3 1451	Pot 4 1407	Pot 5 1464	Pot 6 1444	Pot 7 1427
^{89}Sr	0.39	0.064	—	0.025	0.018	0.15	0.028	0.14	0.11
^{91}Y	0.46	0.35	0.154	0.159	0.096	0.593	—	—	—
^{131}I	1.6	—	0.965	0.492	0.567	—	—	—	—
^{136}Cs	30	30	11.6	2.78	3.98	45.4	9.58	53.0	44.8
^{140}Ba	0.81	0.56	0.356	0.307	0.261	0.971	0.320	1.09	0.829
^{141}Ce	0.76	0.65	0.523	0.490	0.443	0.971	0.515	1.16	0.891
^{144}Ce	0.67	—	0.624	0.599	0.636	0.617	0.617	0.614	0.628
^{147}Nd	0.917	—	0.917[a]	0.917[a]	0.917[a]	0.917[a]	0.917[a]	0.917[a]	0.917[a]
^{156}Eu	11.1	—	—	—	—	10.6	13.0	8.16	11.7

[a]Nuclide ^{147}Nd is taken to be the standard; its R-value is assumed to be 0.917.

the previous section of this report, samples bearing the greatest concentration of refractory radioactive elements also show the greatest amount of thermal decomposition.

Due to the relatively small number of samples and their spatial distribution these results may not be representative of the rubble zone as a whole. There is, however, no indication of any gross difference between dolomite and alluvium in the retention in rock melt of volatile and refractory species, even though the minimum melting point of MgO and CaO is much higher than the melting range for common silicate rocks (2600°K as compared to 1500°K for silicates).

Data on ^{131}I are particularly interesting. Normally, in underground detonations in tuff or alluvium, less than 20% of the ^{131}I formed is retained in the melt with the refractory fission products. In three Handcar samples, however, 31%, 35%, and 60% of the total formed was retained with ^{147}Nd. These samples were taken over a very narrow range of depths (1451, 1452, and 1455 ft) but, on the basis of the relative amounts of ^{89}Sr, ^{91}Y, ^{136}Cs, ^{140}Ba, ^{141}Ce, ^{144}Ce, and ^{147}Nd, they are good diagnostic samples. There is no reason to believe that they represent an anomalous sample of the Handcar debris. We infer from these data that in the Handcar carbonate medium, the Te, Sb, and Sn precursors of ^{131}I are associated with refractory fission products to a significantly larger extent than they usually are in silicate rocks.

WATER-LEACHABILITY OF HANDCAR DEBRIS

The fractions and kinds of radioactive isotopes that can be leached out of Handcar-like rubble is of considerable interest to those involved with Plowshare

applications. Although it was expected that these measurements had been compromised by large amounts of water poured into the Handcar rubble during the postshot drilling operation, a leaching experiment was performed on several samples of the Handcar debris and compared with similar results on a sample from alluvium.

All of the samples were leached in a Soxhlet extractor using a fiber filter thimble. Deionized water was used for all the extractions. After extraction, the filter and residue were dissolved and made up to a known volume, and the leach water was made up to a known volume after rinsing the flask with HCl until no activity could be measured in the flask.

After each extraction a known aliquot of solution was counted and the gamma-ray pulse height was analyzed in a standard geometry. By integrating the entire spectrum and using the aliquot factor the "percent activity leached" was calculated:

$$\% \text{ activity} = \frac{A_{H_2O}}{A_{H_2O} A_{\text{Residue}}} (100).$$

Handcar Leach Sample 1

A 5.7-g sample was ground with mortar and pestle. This sample was not dried before grinding and small pebbles remained (1/8-1/4 in.). It was leached for 8-1/2 hr. About 0.01% of the activity showed up in the leach water.

From gamma-ray analysis the most prominent species in H_2O was ^{124}Sb; Ba-^{140}La did show up. The Zr-^{95}Nb did not show up in the leach water, although it was evident in the solid residue.

Handcar Leach Sample 2

This sample was dried and ground in a pica mill; 3.0 g of the material was leached for 16 hr. About 0.58% of the activity showed up in the leach water. The nuclides present were the same as in sample 1.

Alluvium Leach Sample 4

This sample was dried and ground in a pica mill; 3.3 g was leached for 16-1/2 hr. About 1.6% of the activity showed up in the leach water.

From gamma-ray analysis the most prominent nuclide in the water was ^{124}Sb plus possibly a small amount of Ba-^{140}La. The Zr-^{95}Nb did not show in the water, although it was present in the solid residue.

Taken at face value, these results indicate that the dolomite debris is less leachable than alluvium debris. Until this experiment has been performed on samples which have not been exposed to water, however, the results cannot be taken seriously.

GAS SAMPLING AND ANALYSIS

J. Cowles, R. Crawford, F. Momyer

Gas Recovery

After completion of the postshot drilling and core recovery, 1342 ft of 4-in.-i.d. casing was lowered into the existing 10-in. postshot drill hole (U10b PS #1A). The lower 40 ft of this casing was

punctured with 1-in.-wide by 1-ft-long shots for a total perforation area approximately equal to two inside cross-sectional areas of the pipe.

A valve was welded to the top of the casing and a piping system was constructed at the surface so as to permit drawing of gas from the center 4-in. casing and pumping it into the surrounding annulus as shown in Fig. 31. The β, γ monitor filtered a portion of the gas stream and recorded gross β, γ activity of the particulate. The ^{133}Xe gamma peak was obtained from a NaI sensor downstream of the charcoal-impregnated filter paper. The radioactivity readings were relative and did not indicate absolute concentrations. A Davis combustible gas analyzer was standardized with mixtures of CO in air so 10% CO would give a reading of 75% of explosive limit. The sample bottles were 1-ft^3 evacuated oxygen tanks with valves and fittings at both ends. One end of the tanks was connected to the sampling stream, the other end to evacuated 1-liter flasks. It was intended that these 1-liter aliquots of the samples be valved off and recovered separately for analysis of chemical composition of the samples.

The rupture disks were present to protect the system and the drill casings against pressure pulses >25 psi. If the disks blew out, remote-control bore valves could be used to seal the system. The inlet and outlet flows of the

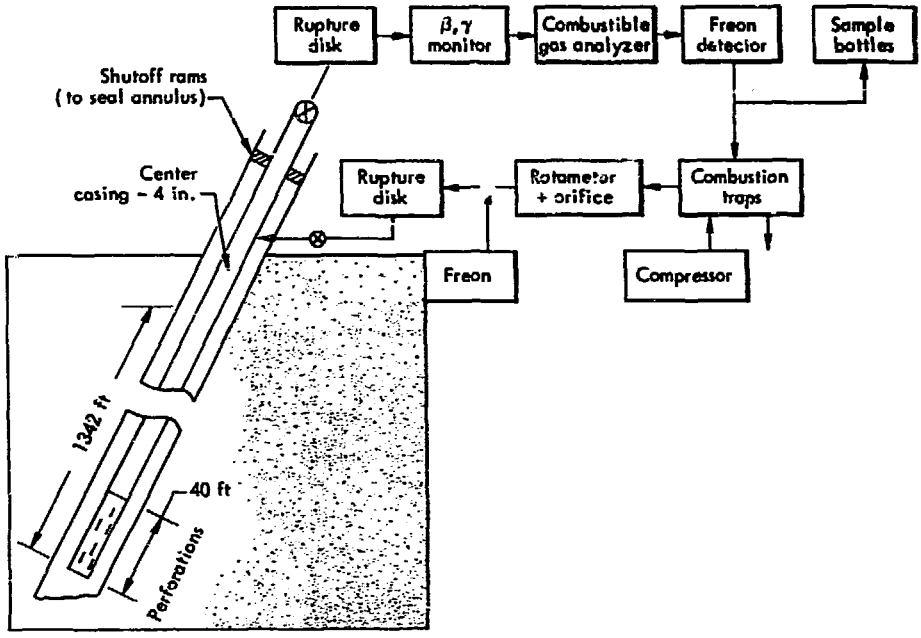

Fig. 31. Handcar gas-sampling system.

compressors were bubbled through water traps to prevent spread of flames due to ignition of combustible gas in the compressor.

When pumping was first started on the center casing, a 16-in.-Hg vacuum was formed within the pipe in 6 min. The vacuum held at 16-in. Hg with no noticeable change on two gauges for over 2 hr. The flow was then reversed and air was pumped into the center 4-in. casing. The casing was pressurized to 7 psig in about 5 min. No additional pressure increase was noted although pumping was continued for half an hour. It was surmised that the bottom of the casing was about 50 ft below the level of drilling mud left in the hole. Thus the top of the perforated section was about 10 ft below the mud, and 7 psig was required to force air through the perforations.

A wire-line probe later showed a water surface at 1291 ft (the bottom of the casing was about 1342 ft). Twenty 13.5-g explosive charges on a wire line were fed into the casing to perforate the wall between 1265 and 1270 ft; then 40 charges were fired between 1225 and 1235 ft. Subsequent pumping tests indicated the hole was unplugged and that gas could be pumped from the casing.

The explosive perforations occurred within the void at the top of the Handcar chimney, which was at a 5-in.-water vacuum relative to atmospheric pressure (December 22, 1964, 2 to 8 p.m.).

During the sampling run, gas was pumped into the annulus. About 0.1% Freon was injected into the gas stream. It was planned to pump gas until the radiation, combustible gas, and Freon sensors indicated steady-state conditions were prevailing. Steady state would be indicated by no additional increase of signal from the sensors after pumping for a few minutes.

When the run was started, the combustible gas meter soon stabilized at 4% of the explosive limit. A high gamma level was sensed by the xenon peak detector and the gross β, γ particulate detector. A hand-held radiation meter read 3 mR when placed briefly in the gas stream. No Freon return was observed. Portable gas analyzers used by REECo Radsafe personnel indicated a 20% CO_2 content in the gas. These conditions prevailed without significant change for 6 hr, at which point pumping was terminated.

Six hourly 1-ft^3 gas samples were obtained and labeled 1H1-1H6. A final set of six 1-ft^3 samples was taken just prior to the termination of the run and labeled 1F1-1F6. Twelve hours after pumping had ceased, twelve 1-ft^3 samples were drawn from the top of the 4-in. casing and labeled residual gas.

Analysis for Nonradioactive Gases

The 1-liter aliquots taken in the field from samples 1H1-1H6 were analyzed by mass spectrometry. Subsequent sampling of the 1-ft^3 bottles showed that the gases found in the smaller containers were not representative, therefore all results reported here are for gases taken from the 1-ft^3 cylinders.

Gross analyses of the gases were carried out by standard techniques on a CEC 21-103C and analytical mass spectrometer.

Trace analyses of the gases were performed by gas chromatography.

Table 9 contains the combined results of gross and trace analyses on Handcar gases. Table 10 contains the same information after normal air, based on the oxygen content of the samples, has been removed. Compared to normal air, oxygen was depleted in these samples as shown by the residual quantities of N_2 and Ar in Table 10. It is assumed that this O_2-depleted air was present in the cavity at sufficiently early times to permit reactions to consume the oxygen.

Table 9. Nonradioactive Handcar gases. Air and CO_2 determined by mass spectroscopy; CO, H_2, and CH_4 by gas chromatography.

Sample	Gross analyses (vol%)					Trace analyses (ppm)		
	CO_2	Ar	O_2	N_2	Air	CH_4	H_2	CO
1H1[a]	63.6	0.359	7.12	28.8	36.2	399	369	1390
2	65.4	—	—	—	34.4	269	362	1120
3	64.1	0.329	7.00	28.4	35.7	255	360	1270
4[a]	60.8	0.349	7.88	30.7	39.0	294	345	1210
5	64.6	—	—	—	35.2	265	352	1290
6	70.3	—	—	—	29.5	290	412	1340
1F1	76.6	0.220	4.30	18.6	23.1	313	427	1390
2	79.7	—	—	—	20.1	321	438	1340
3	78.1	—	—	—	21.7	309	421	1410
4	79.9	—	—	—	19.9	326	435	1360
5[b]	71.3	—	—	—	28.5	281	386	1210
6[a]	77.9	0.210	4.14	17.5	21.9	309	382	1370
Residual:								
1	0.15	0.92	20.79	78.1	99.9	—	—	—
2	1.05	0.93	20.24	77.8	99.0	—	—	—

[a]Approximately half of the sample was withdrawn for radiochemical gas analysis prior to these determinations.

[b]Sample container probably leaked; its pressure was 73 cm Hg, while all others were about 65 cm Hg.

Table 10. Handcar chimney gas composition. Air based on oxygen removed.

Sample	Gross analyses (vol%)			Trace analyses (ppm)		
	CO_2	N_2	Ar	CO	H_2	CH_4
1H1	96.2	3.37	0.06	2110	557	452
1H3	96.3	3.43	0.03	1900	540	382
1H4	97.4	2.22	—	1930	552	469
1F1	96.0	3.22	0.03	1740	534	391
1F6	97.1	2.57	0.02	1710	475	384

Normal air was then subsequently mixed with the cavity gases during chimney collapse and at reentry.

The amount of O_2 consumed under these assumptions was about 5×10^5 moles. Iron associated with the explosive was partially responsible for this usage of O_2. The total amount of iron close to the explosion was about 9.4 metric tons or 1.7×10^5 moles. This could have consumed at most about 1.3×10^5 moles of O_2 according to the reaction

$$4Fe + 3O_2 \longrightarrow 2Fe_2O_3.$$

The presence of CO and traces of H_2 and CH_4 in the gas indicates that high temperature reactions between Fe, CO_2, and H_2O occurred. However, there does not seem to have been sufficient metal near the explosive to explain the consumption of oxygen as well as the formation of H_2, CO, and CH_4. It is possible that the Handcar dolomite contains a trace of free carbon. A concentration of about 0.05 wt% free carbon would be sufficient to account for the discrepancies discussed above.

Analysis for Radioactive Gases

Radiochemical analyses were performed on the three gas samples designated 1H1, 1H4, and 1F6. These samples were taken at the start, at the end of the third hour, and at the end of the sixth hour of circulation of cavity gas through the sampling train.

In each sample $^{14}CO_2$, ^{14}CO, ^{37}Ar, ^{39}Ar, ^{85}Kr, ^{133}Xe, and ^{131m}Xe were counted in the corresponding chemical fractions. Separation of these fractions was by gas chromatography.

For krypton and xenon, measured amounts of inactive carriers were added to measured aliquots of gross sample and reseparated. All other species of interest were separated from the gross sample without addition of carrier, and the specific activity of the radionuclide in its naturally occurring isotopic species was determined.

For convenience, all results were normalized to 1 liter STP of sample after air based on oxygen was removed. The aforementioned determinations of chemical composition were required at this point; e.g., for krypton and xenon, the ratio of gross sample to reduced sample, and for other species, the volume percent of the species per liter of reduced sample.

Chemical purity of fractions was checked by mass spectrometry. Corrections were applied where necessary, although these were nearly always negligible. Results are given in Table 11.

A quantity which is of radiochemical interest is the isotopic ratio for compounds containing ^{14}C. Table 12 lists these results in terms of specific activity (dpm per mole) for these species.

The physical model used as a guide to interpretation of the results is as follows: Initially the nuclear explosion produced a spherical region lined with molten rock and filled with vaporized rock and device debris. This cavity rapidly expanded to the ultimate cavity radius by radial displacement of the medium outside the molten layer. It is assumed that mixing of gases was complete within this cavity, and that in cases where a given isotope existed as several chemical species, isotopic ratios were the same for all

Table 11. Handcar radiochemical gas analysis results. Equivalent fissions[a] or dpm at zero time per liter (STP) of sample after air based on oxygen is removed.

Sample	1111	1114	1116	Average
Time	Start of circulation	After 3 hr	After 6 hr	—
^{85}Kr (fissions)	3.75×10^{15} (0.7)[b]	3.70×10^{15} (1.1)[b]	3.70×10^{15} (1.2)[b]	3.72×10^{15} (0.8)[b]
^{133}Xe (fissions)	7.69×10^{15} (1.4)	7.02×10^{15} (2.5)	7.87×10^{15} (6.9)	7.53×10^{15} (3.3)
^{131m}Xe (fissions)	6.92×10^{15} (1.4)	6.12×10^{15} (1.0)	5.84×10^{15} (3.1)	6.29×10^{15} (4.7)
^{37}Ar (dpm)	5.66×10^{7} (0.5)	6.03×10^{7} (1.1)	6.64×10^{7} (1.0)	6.11×10^{15} (4.9)
^{39}Ar (dpm)	6.84×10^{2} (1.8)	7.77×10^{2} (1.5)	—	7.29×10^{2} (6.9)
^{14}CO (dpm)	3.03×10^{1} (0.2)	2.72×10^{1} (0.4)	2.59×10^{1} (0.2)	2.78×10^{1} (4.4)
$^{14}CO_2$ (dpm)	7.92×10^{3} (4.9)	6.64×19^{3} (4.0)	6.69×10^{3} (8.3)	7.08×10^{3} (5.6)

[a]For fission product gases, the tabulated number is the number of fission events equivalent to the observed gaseous activity.

[b]Numbers in parenthesis are estimated standard errors expressed in percent of the mean values. For the individual samples these values do not include errors in chemical composition.

Table 12. Handcar average totals of gaseous radionuclides, based on ^{85}Kr production expected from a fission yield of 10.1 kt.

Radionuclide	Average total	Equivalencies
^{85}Kr	6.44×10^{24} fissions	10.1 kt (normalization point)
^{133}Xe	2.76×10^{24} fissions (3.3%)	20.4 kt
^{131m}Xe	3.72×10^{24} fissions (4.7%)	17.1 kt apparent[a] 20.6 kt decay-corrected
^{37}Ar	2.30×10^{16} dpm^0 (4.9%)	1.0×10^{3} Ci/kt
^{39}Ar	4.59×10^{9} dpm^0 (6.9%)	1.2×10^{-2} Ci/kt
CO	1.06×10^{10} dpm^0 (4.4%)	9.0×10^{-4} of ^{14}C tracer
CO_2	2.69×10^{12} dpm^0 (5.5%)	0.228 of ^{14}C tracer
Average volume of gas mixed with ^{85}Kr after air removed	3.79×10^{8} liters STP (0.8%)	~10 cavity volumes STP

[a]The radionuclide ^{131m}Xe at sampling time is at 83% of its maximum extrapolated activity level due to the appreciable half-life of the ^{131}I precursor (8.0 days).

species. For instance, $^{14}C/C$ was the same in carbon dioxide, carbon monoxide, methane, and any other compound of carbon.

Geophone records indicate that the cavity collapsed between 14 and 35 sec after the detonation. During this period some of the heat energy of the cavity materials is utilized to increase the temperature of the chimney rock, releasing carbon dioxide and water with a corresponding rapid cooling of the system.

As a first approximation it is assumed that rates of chemical reactions, including particularly isotopic exchange reactions, drop essentially to zero as a result of this cooling. Reactions such as $^{14}CO_2 + CO \rightarrow {}^{14}CO + CO_2$ are assumed to occur negligibly after collapse. Dilution of the $^{14}CO_2$ with carbon dioxide is possible until temperatures drop below those necessary to release CO_2 from the dolomite. Carbon monoxide, produced by reactions of CO_2 with reducing agents (principally iron), is essentially free from such dilution effects. The assumption of low ^{14}C exchange rates after cooling is more likely valid for CO than for CO_2, since the latter could exchange with carbonate minerals on the surface of the exposed dolomite. This likelihood is enhanced by the presence of water, a large amount of which was added to the chimney during drilling operations. One of the goals of the gas analysis investigation for Handcar was to search for evidence relative to these assumptions, and if possible to evaluate the effects of exchange and dilution upon the chimney gas chemistry.

The following data are pertinent to interpretation of the results: 5.30 Ci (±1.0%), or 1.177×10^{13} dpm^0 (±1.0%), of ^{14}C as $BaCO_3$ was loaded as symmetrically as possible in eight packets around the device. This amount is about 50 times that expected to be produced in the explosion. About 10^5 gal, or 2×10^7 moles, of H_2O was introduced into the emplacement hole during preshot drilling. About 1.5×10^6 gal, or 3×10^8 moles, of H_2O was introduced to the postshot reentry hole. The radiochemical device yield was 10.1 ± 1 kt. The present best estimate of cavity radius from preasurization measurements is 20.6 ± 0.5, corresponding to a void volume of 3.6×10^7 liters.

Totals of Gaseous Species

Recent experience has suggested that essentially all of the rare-gas fission products produced in a contained nuclear explosion mix with the chimney gas. This appears to be true regardless of chimney collapse time, indicating that possible entrapment of precursors in solidified melt is not an important consideration.

However, this experience is based upon experiments performed with nuclear explosions in silicate rock. Gas in the silicate rock surrounding the chimney (mostly air) enters the chimney to fill the partial vacuum created by steam condensation. Any gaseous material injected into the formation by initially high cavity pressures would be flushed back into the chimney. In the case of Handcar, on the other hand, CO_2 was generated in amounts sufficient to carry cavity gases into the permeable formation and to effectively remove them from the chimney region. The very low water content of the medium, and the fact that the generation of CO_2 by the thermal decomposition of dolomite continued for some time after detonation (perhaps several hours), would seem to indicate that this was the case.

So that totals of species can be estimated in any such experiment, a known amount of a gaseous species which is mixed well with the gaseous device debris can be used as a device fraction indicator. No such species existed on the Handcar experiment. As a second choice it is

possible to calculate the expected total of a fission product gas from the experimentally determined fission yield of the explosive. Perhaps the most useful such fission product is ^{85}Kr, which is produced from decay of the 3-min ^{85}Br, and is, therefore, essentially all present at about 10 min after detonation. Since we know the amount of ^{85}Kr which would be produced by the Handcar device, we can use this species as a device fraction indicator to obtain totals of other species with which the ^{85}Kr has mixed. These totals should be considered as lower limits due to possible physical fractionation, especially at early times when high-pressure cavity gases could escape to the formation before complete growth and mixing of the ^{85}Kr. Average values of the totals of species based upon ^{85}Kr are listed in Table 12.

With these data, comments, and cautionary notes in mind, the results for each of the chemical species separated are discussed individually below.

Carbon Dioxide

Assuming $^{14}C/C$ to be the same at sampling time in all carbonaceous species containing significant amounts of ^{14}C (i.e., CO_2 and CO_3), the average of 1.64×10^5 dpm^0 (±10.9%) of ^{14}C per mole of CO_2 implies exchange with 7.19×10^7 moles of carbon or an equivalent 8.6×10^9 g of dolomite.

If one could equate the carbon with which the tracer exchanged with that in the melt and vaporization zone, this would correspond to 550 tons of dolomite melted or vaporized per kiloton of yield. The amount of carbon 14 as $^{14}CO_2$ that mixed with ^{85}Kr was about 23% of the total ^{14}C loaded. Only about 10% of this material was found as gas in the chimney at reentry two months after the shot. Evidently some of the ^{14}C was injected at early times into the formation without mixing with the ^{85}Kr, or was included in some solid-state materials, or both.

It seems probable that $^{14}CO_2$ and ^{14}CO present in the chimney immediately following detonation could have been displaced away from the chimney by the continued generation of CO_2 relatively free of ^{14}C. The ^{85}Kr, because of its growth period which is on the order of 10 min, would have been displaced to a lesser extent than the ^{14}C but nevertheless would be depleted in the chimney region.

Unfortunately, one cannot assume that these observations apply to conditions existing before reentry to the cavity. The addition of 3×10^8 moles of water to the postshot hole would be expected to result in slaking of CaO and MgO and subsequent rapid reconversion of CO_2 to carbonates.

In addition, exchange of ^{14}C in a CO_2-water-carbonate system would be expected to be rapid. The exchange between carbonates and gaseous CO_2 in a humid environment is a common problem in counting ^{14}C as solid carbonates. Appreciable exchange with carbonates not originally in the melt zone therefore undoubtedly occurred prior to sampling, and the 550 tons of melt per kiloton of yield must be considered a poor upper limit.

Carbon Monoxide

The activity of ^{14}C per mole of CO sampled is 3.27×10^5 dpm^0 ±3.8%. If

this specific activity is representative of original carbon in the cavity, there was 340 tons of dolomite per kt of yield in the melt and vapor zone. Assuming the total ^{14}CO found mixed with ^{85}Kr and ignoring the possibility of exchange, one can estimate that 9×10^{-4} of the ^{14}C tracer was as CO in the original cavity, implying that the same fraction of the available carbon went to form CO.

Total Gas Volumes

Since essentially all of the gas present in the Handcar environment was CO_2 there are at least three methods of obtaining an estimate of the total volume of gas generated by the detonation. These have been discussed previously but will be summarized here.

From the amount of ^{14}C tracer loaded with the device and the observed $^{14}CO_2$ concentration in the CO_2 gas recovered, an estimate of 7.2×10^7 moles for the total CO_2 production was obtained. This value is an upper limit due to the possibility of radiochemical exchange. By comparison, a similar calculation using the ^{14}C content of CO indicated about half this much gas or 3.6×10^7 moles was generated. The amount of gas with which the ^{85}Kr was mixed (assuming uniformity with observed concentrations from the chimney region) was 1.7×10^7 moles. These quantities are summarized in Table 13. It is interesting to note that by using the device fractions measured for refractory device debris and the CO_2 lost from these diagnostic samples, Taylor obtains a total CO_2 release of about 2.5×10^7 moles, in good agreement with these values (see Part II of this report).

Table 13. Total amount of CO_2 produced in Handcar, calculated by three different methods.

Calculational basis	Total moles of CO_2
$^{14}CO_2/CO_2$	7.2×10^7
$^{14}CO/CO$	3.6×10^7
$^{85}Kr/CO_2$	1.7×10^7
Average	4.2×10^7

If one takes the average production as 4×10^7 moles and assumes a formation permeability of 4% (Ref. 4), it is possible to construct an estimate of the volume of this expanded gas bubble relative to that of the chimney. A sketch of this relationship is presented in Fig. 32. Spherical symmetry, atmospheric pressure, and a temperature of 50°C were assumed.

Argon

Based on the use of ^{85}Kr as a device fraction indicator, the total production of ^{37}Ar is seen to be about 10^4 Ci, while total ^{39}Ar is about 120 mCi. These isotopes are produced principally in the dolomite through interactions with escaping neutrons, according to the reactions $^{40}Ca(n,\alpha)^{37}Ar$, $^{42}Ca(N,\alpha)^{39}Ar$, or $^{39}K(n,p)^{39}Ar$. Although preshot estimates of the totals expected are about an order of magnitude greater than those measured, the lack of agreement is not considered serious due to the uncertainties involved in the calculations and the possibility that argon was swept into the formation at early times, preventing it from mixing with the ^{85}Kr.

Fission Product Gases

Because ^{85}Kr has been used to obtain totals of species in the gas, only the

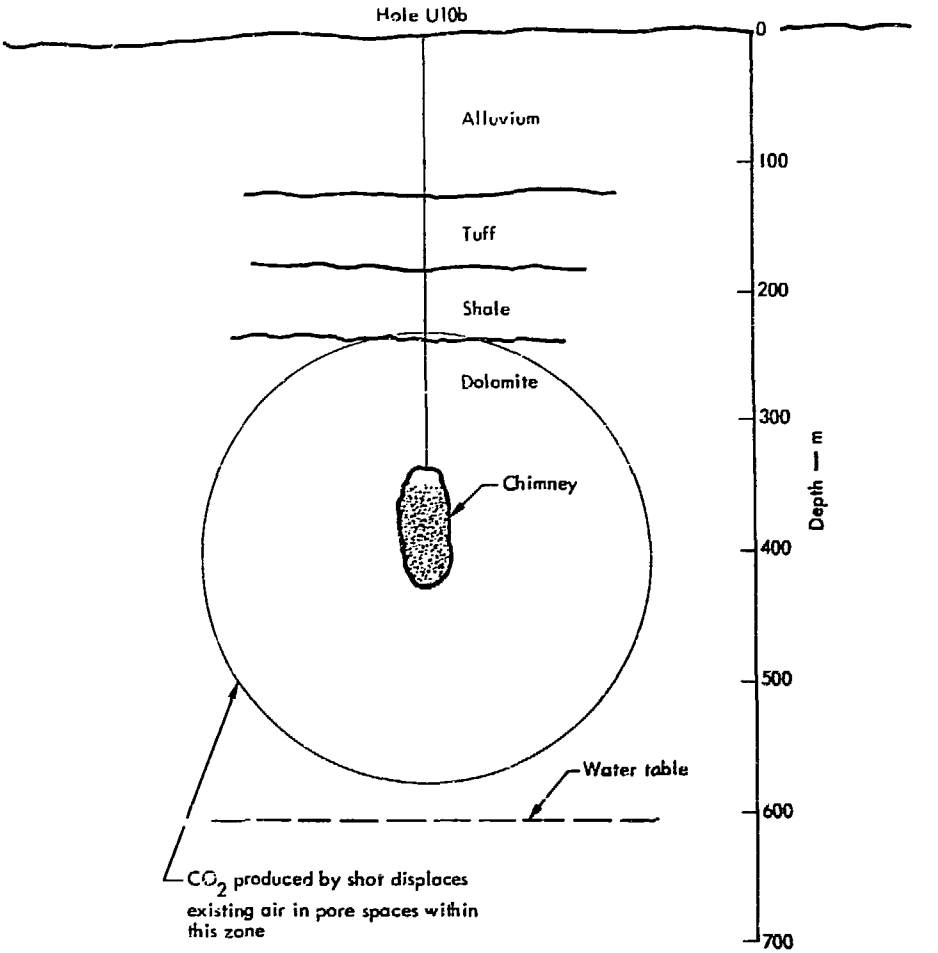

Fig. 32. Possible disposition of the calculated 4×10^7 moles of CO_2 produced by the Handcar explosion.

relative amounts of the fission products are of significance here. Examination of Table 12 reveals that the equivalent fission yields obtained for ^{133}Xe and ^{131m}Xe are about twice the assumed yield. No completely satisfactory explanation is available for this disparity. Depressurization of the chimney most probably occurred shortly after collapse. Since the ^{85}Kr growth is essentially complete in the first 10 minutes, and since our recent experience suggests that the krypton will mix with the gas, depressurization is a probable explanation for the removal of krypton from the chimney.

Xenon isotopes exist primarily as precursors at these early times. Growth of ^{133}Xe requires several days, while ^{131}Xe growth is not complete until several months after detonation. The similar equivalent fission yields deduced for these isotopes indicates absence of fractionation effects. Since fractionation would result if depressurization was occurring during or after ^{133}Xe growth, this observation supports the assumption of rapid depressurization. However, if it is assumed that 100% of the xenon growth mixes with the gas, then the equivalent of about 4.5 chimney volumes of gas at atmospheric pressure is required to give the observed concentrations. This volume of gas is not likely to be available through diffusion processes, and neither can we assume that it was lost by depressurization since fractionation did not occur.

This anomaly in regard to the xenon can be rationalized in a number of ways involving assumptions of diffusion and effusion rates, fractions in the gas, effects of slaking as a result of addition of water, pure coincidence, etc. None of these possible explanations can be supported by experimental measurement or past experience. On the basis of sampling at a single time postshot, and in consideration of other uncertainties mentioned previously, there is nothing to be gained by further conjecture.

Part IV. Conclusions

1. The Handcar experiment demonstrated that large quantities of noncondensable carbon dioxide are generated by a nuclear detonation in a carbonate medium. No serious containment problems resulted, although the highly porous medium allowed the Handcar chimney to depressurize rapidly. Since, in this respect, the Handcar dolomite may not be characteristic of carbonate formations of interest for Plowshare underground engineering applications, possible containment problems should be carefully considered for future experiments of this kind, particularly in nonporous rock.

2. The cavity radius is about 10% less and the chimney height about 27% less than would be expected in granite. Evidently the carbon dioxide generated by the nuclear explosion did not play a major role in cavity formation.

3. We can predict the strength of strong shock, in the hydrodynamic region. We do not have an understanding of the plastic, crushed, and near-elastic region. The difficulty may be experimental or theoretical, or both. This latter region is of interest for some underground applications and more work needs to be done in developing an understanding of it.

4. Close in, the seismic waves generated, in terms of peak values of particle velocities, are comparable to those generated in competent tuff, whereas far out they are about half the magnitude of those in competent tuff. Considering the porosity, compressional velocity, and bulk density of the rock, this result is surprising.

5. *Differences of seismic propagation* caused by alluvium in one direction and hard rock in the other have been reasonably well handled by the TENSOR code. Handcar has not provided a good test because the effect was too small. This capability will grow with time and will prove useful in evaluating seismic damage in specific applications.

6. Samples of the chimney gas obtained six weeks after detonation were 30-40% air and 70-60% carbon dioxide, with trace quantities of methane, hydrogen, and carbon monoxide.

7. About 2×10^9 g ($(9 \pm 7) \times 10^8$ liters or $(3 \pm 2) \times 10^7$ ft^3 STP) of CO_2 was produced by the heat of the explosion. This required about 20 ± 5% of the total explosive energy.

8. Although data are fragmentary and the samples taken may not be representative of the rubble zone as a whole, there appears no gross difference between dolomite and tuff or alluvium in the retention of volatile radioactive species.

9. Results obtained in leaching experiments using Handcar debris may have been compromised by the large quantities of water introduced during postshot drilling. Taken at face value these results indicate that dolomite may be less leachable than alluvium debris.

10. Specific activity of ^{14}C implies exchange with the equivalent of 550 tons of dolomite per kiloton yield based on CO_2 and 280 tons of dolomite per kiloton based on CO.

11. Total production (based on ^{85}Kr) of ^{37}Ar and ^{39}Ar by neutron activation of the calcium or potassium in the soil was measured as 10^3 Ci and 120 mCi of these materials, respectively. These values may be lower limits if significant depressurization occurred prior to mixing with ^{85}Kr.

12. Ratios of the fission product gases imply rapid depressurization of the Handcar chimney. If ^{85}Kr is assumed to be 100% in the gas phase, then about 90% of this gas resides outside the chimney region. The large quantities of CO_2 generated by thermal decomposition of the dolomite for as long as several hours after the detonation may have swept significant fractions of cavity gas into the formation during the early postdetonation period. Indications of the Xe isotopes are that this depressurization was essentially ended prior to appreciable growth of ^{133}Xe, which is on the order of a day.

References

1. C. R. Boardman, D. D. Rabb, and R. D. McArthur, "Responses of Four Rock Mediums to Contained Nuclear Explosions," J. Geophys. Res. 69, 3457 (1964).
2. L. S. Germain and J. S. Kahn, Phenomenology and Containment of Underground Nuclear Explosions, Lawrence Radiation Laboratory, Livermore, Rept. UCRL-50482 (1968).
3. J. T. Cherry, D. B. Larson, and E. G. Rapp, "A Unique Description of the Failure of a Brittle Material," Int. J. Rock Mech. Min. Sci. 5, 455 (1968).
4. C. R. Boardman, G. L. Meyer, and D. D. Rabb, Macrodeformation Resulting from the Handcar Event, Lawrence Radiation Laboratory, Livermore, Rept. UCRL-50149 (1966).
5. L. A. Rogers, Shock Compression of Several Rock Types, Lawrence Radiation Laboratory, Livermore, Rept. UCRL-12027 (1964).
6. F. Holzer, "Calculation of Seismic Source Mechanisms," Proc. Roy. Soc. (London) Ser. A, 290, 408 (1966).
7. G. C. Werth and R. F. Herbst, "Comparison of Amplitudes of Seismic Waves from Nuclear Explosions in Four Mediums," J. Geophys. Res. 68, 1463 (1963).
8. F. M. Sauer, "Ground Motion from Underground Nuclear Explosions," Ch. IV-2 in Nuclear Geophysics, Part Four, Empirical Analysis of Ground Motion and Cratering, Defense Atomic Support Agency Rept. DASA-1285(IV) (1964).
9. J. T. Cherry and W. R. Hurdlow, "Numerical Simulations of Seismic Disturbances," Geophysics 31, 33 (1966).
10. F. H. Smythe and L. H. Adams, "The System Calcium Oxide-Carbon Dioxide," J. Am. Chem. Soc. 45, 1167 (1923).
11. D. L. Graft and J. R. Goldsmith, "Dolomite-Magnesian Calcite Relations at Elevated Temperatures and CO_2 Pressures," Geochim. Cosmochim. Acta 1, 109 (1955).
12. R. I. Harker and O. F. Tuttle, "Studies in the System CaO-MgO-CO_2, Pt. I, The Dissociation of Calcite, Dolomite, and Mangesite," J. Am. Sci. 253, 209 (1955).
13. R. I. Harker and O. F. Tuttle, "Studies in the System CaO-MgO-CO_2, Pt. II, Limits of Solid Solution Along the Binary Join $CaCO_3$-$MgCO_3$," J. Am. Sci. 253, 274 (1955).
14. J. R. Goldsmith and H. C. Heard, "Subsolidus Phase Relations in the System $CaCO_3$-$MgCO_3$," J. Geology 64, 45 (1961).

15. J. F. Lakner, Treatment of Dolomite and Its Decomposition Products Under Pressure and Temperature, Lawrence Radiation Laboratory, Livermore, document consisting of unclassified portions of the classified Repts. UCRL-7047 (pp. 27-38), UCRL-7142 (pp. 8-16), and UCRL-7213 (pp. 26-35) (1964). (Declassification of these portions of the reports is authorized in Topic 5.1.1 of CG-UF-1 by J. S. Stuart of the LRL Livermore Classification Office.)

16. B. McBride, S. Heimel, J. Ehlers, and S. Gordon, Thermodynamic Properties to 6000°K for 210 Substances Involving the First 18 Elements, NASA Lewis Research Center, Cleveland, Ohio, Rept. NASA SP-3001 (1963).

17. H. L. Schick, editor, Thermodynamics of Certain Refractory Compounds (Academic Press, New York, 1966).

18. S. P. Clark, Jr., editor, Handbook of Physical Constants, Geological Society of America, Memo 197 (1966).

19. K. K. Kelley, Contributions to the Data on Theoretical Metallurgy, U. S. Bur. Mines Bull. 584 (1960).

20. F. J. Krieger, On the Thermodynamics of Calcite, The RAND Corporation, Santa Monica, Calif., Memorandum RM-4590-PR (1965).

21. N. M. Saha and D. N. Srivastava, A Treatise on Heat (The Indian Press, Ltd., Allahabad and Calcutta, 1950).

22. R. W. Taylor, E. L. Lee, and J. H. Hill, Interpreting the Chemical Results of the Gasbuggy Experiment, Lawrence Radiation Laboratory, Livermore, Rept. UCRL-72112 Preprint (1969). (Published in Proceedings of the ANS Topical Meeting on Engineering with Nuclear Explosives, Las Vegas, Nevada, Jan. 14-16, 1970.)

Printed in USA. Available from the National Technical Information Center, National Bureau of Standards, U. S. Department of Commerce, Springfield, Virginia 22151